Talanta 259 (2023) 124548

Contents lists available at ScienceDirect

Talanta

journal homepage: www.elsevier.com/locate/talanta

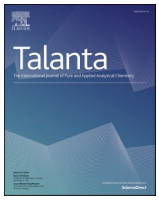

Recent advances in electrochemical nanomaterial-based aptasensors for the detection of cancer biomarkers

Masoud Negahdary [*], Lúcio Angnes [**]

Department of Fundamental Chemistry, Institute of Chemistry, University of São Paulo, Av. Prof. Lineu Prestes, 748, São Paulo, 05508-000, Brazil

ARTICLE INFO

Keywords:
Cancer diagnosis
Biomarkers
Aptamer
Aptasensor
Nanomaterials
Bioanalysis
Bioelectrochemistry

ABSTRACT

New technologies have provided suitable tools for rapid diagnosis of cancer which can reduce treatment costs and even increase patients' survival rates. Recently, the development of electrochemical aptamer-based nanobiosensors has raised great hopes for early, sensitive, selective, and low-cost cancer diagnosis. Here, we reviewed the flagged recent research (2021–2023) developed as a series of biosensors equipped with nanomaterials and aptamer sequences (nanoaptasensors) to diagnose/prognosis of various types of cancers. Equipping these aptasensors with nanomaterials and using advanced biomolecular technologies have provided specified biosensing interfaces for more optimal and reliable detection of cancer biomarkers. The primary intention of this review was to present and categorize the latest innovations used in the design of these diagnostic tools, including the hottest surface modifications and assembly of sensing bioplatforms considering diagnostic mechanisms. The main classification is based on applying various nanomaterials and sub-classifications considered based on the type of analyte and other vital features. This review may help design subsequent electrochemical aptasensors. Likewise, the up-to-date status, remaining limitations, and possible paths for translating aptasensors to clinical cancer assay tools can be clarified.

1. Introduction

Cancer is explicitly considered the uncontrolled growth of cells that can occur in all organs and lead to death by disrupting the proper functioning of cells [1–3]. According to recent figures from the World Health Organization (WHO), cancer is the leading cause of death (approximately 10 million expire annually [4,5]. The most common cancers are related to the breast, lung, colon, rectum, and prostate [4,6,7]. Frequent factors, such as genetics, improper nutrition, smoking, drinking, and environment, turn normal cells into cancerous ones [8–11]. In addition, active infections (such as hepatitis and human papillomavirus (HPV) infections) and insufficient physical activity are other cancer risk factors [10,12,13]. Early detection of cancers is vital since it can significantly increase the five-year survival rate. Imaging tests such as CT scans, MRI, and PET scans are often highly sensitive in detecting cancer [14,15]. However, these tests can also produce false-positive results, meaning they may indicate the presence of cancer when there is none. Biopsy is considered to be the gold standard for cancer diagnosis, as it can provide a definitive diagnosis with a high degree of accuracy [16,17]. However, biopsies can be invasive and may not be appropriate for all patients [18]. Blood tests are another option for cancer detection, and some tests can be highly sensitive [19]. Genetic testing can also be highly sensitive in detecting certain types of cancer, particularly those caused by genetic mutations [20,21]. However, genetic testing is generally used for people who have a family history of cancer or other risk factors for the disease. In summary, the desirable sensitivity for cancer detection varies depending on the specific cancer and the method used for detection, and a combination of different tests may be needed to accurately diagnose and monitor cancer. Principally, cancer diagnostic biomarkers consist of biomolecules, and any slight changes in their concentration can be used for early diagnosis and even prognosis of various cancers [22–26]. Most cancers generally have specific diagnostic biomarkers [27,28]; therefore, determining cancer biomarkers concentration has a particular and applicable diagnostic advantage. Biosensing platforms are designed as one of the modern biomedical diagnostic tools. The capabilities of biosensors include providing low-cost, portability, repeatability, simplicity, sensitivity, and highly selective diagnostics [27,29–35].

* Corresponding author.
** Corresponding author.
E-mail addresses: mnegahdary@iq.usp.br (M. Negahdary), luangnes@iq.usp.br (L. Angnes).

https://doi.org/10.1016/j.talanta.2023.124548
Received 31 January 2023; Received in revised form 7 April 2023; Accepted 10 April 2023
Available online 11 April 2023

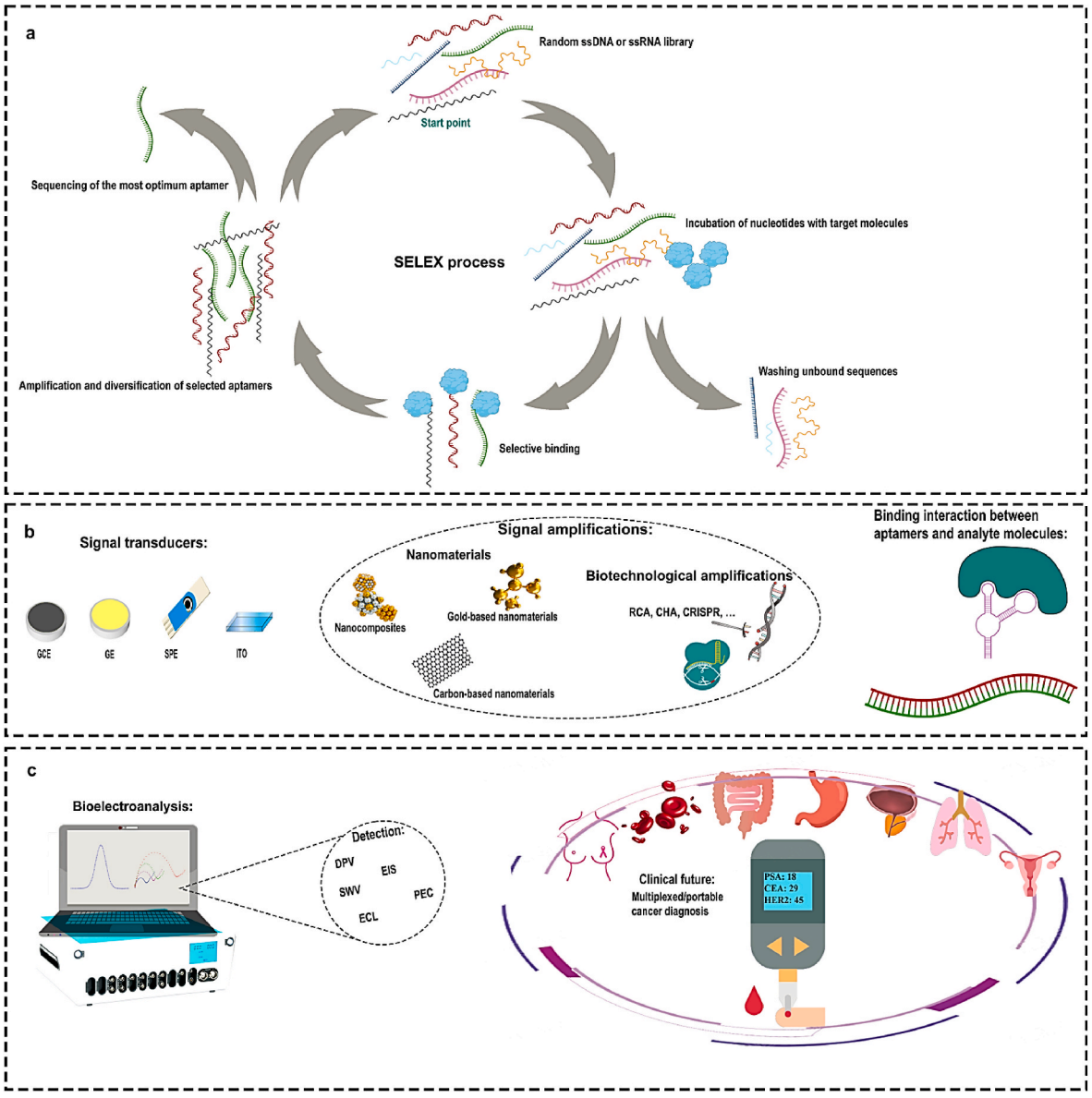

Fig. 1. Schematic illustration of main elements used in electrochemical nanomaterial-based aptasensors for detection of cancer biomarkers; SELEX process for optimized selection of aptamers from a random oligonucleotide library **(a)**; common types of working electrodes (signal transducer: glassy carbon electrode (GCE), gold electrode (GE), screen-printed electrode (SPE), and Indium tin oxide (ITO)), signal amplification methods (application of nanomaterials and biotechnological techniques), and usual types of analyte detection by aptamers including changing conformation and capturing biomarkers and hybridization with complementary nucleotide sequences **(b)**; In electrochemical aptasensors, the absence and presence of different concentrations of the analyte will change the electron transfer rate passed from the working electrode surface, followed mainly through differential pulse voltammetry (DPV), electrochemical impedance spectroscopy (EIS), square wave voltammetry (SWV), PEC, and ECL. Suppose it is possible to commercialize the electrochemical aptasensors to diagnose cancer biomarkers. In that case, it will be accessible to have these diagnostic systems as portable and even diagnose several types of cancer markers simultaneously (multiplexed) **(c)**.

Electrochemical aptasensors in cancer diagnosis have been introduced as a group of biosensors equipped with high-affinity aptamer sequences (as the biorecognition element) against cancer biomarkers [24,36–38]. Aptamers are single-stranded nucleotide (ssDNA or ssRNA) sequences (usually between 10 and 100 mer). Systematic evolution of ligands by exponential enrichment (SELEX) is used to produce diagnostic aptamers. The SELEX process involves several rounds of selection and amplification, starting with a large pool of random oligonucleotides [39,40]. The oligonucleotides are incubated with the target molecule, and those that bind to the target with high affinity are isolated and amplified by polymerase chain reaction (PCR). The resulting pool of amplified oligonucleotides is then subjected to another round of selection, and the process is repeated until a pool of highly specific aptamers is obtained (Fig. 1, a). Aptamers can be bound to a wide range of targets, including small molecules, proteins, whole cells, and even can be hybridized with nucleotide sequences. The binding specificity of an aptamer is determined by its sequence and 3D structure, which can be optimized during synthesis. Aptamers are a promising alternative to antibodies and can detect analytes primarily based on conformational changes [41,42]. Aptamers have important advantages over antibodies, such as smaller size, higher stability, lack of immunogenicity, anticipated design (this feature leads to higher specificity), easier use, and applicability for chemical functionalization [27,28,31,43–45].

Recently, many efforts have been trailed to optimize the performance of aptasensors. One of the most important optimizations in the structure of these biosensors is the use of nanomaterials [30,31,43,46–48]. Due to unique physicochemical properties, such as the increased surface area to volume ratio, nanomaterials provide improved

diagnostic sensitivity [29,49,50]. Usually, nanomaterials can optimize the surface of signal transducers to have an enhanced electroactive surface area for interaction with the biorecognition element and/or can have application as parts of the biorecognition element [30,31,46,51]. The most common types of nanomaterials used in the recent design of aptasensors are gold/carbon-based nanomaterials, which have been preferred due to the several essential advantages (biocompatibility, high conductivity, easy preparation, and environmental stability) [31,52,53].

In addition to nanomaterials, some other signal amplification strategies are employed for aptasensors which can enhance the sensitivity and selectivity and enable the detection of low concentrations of analyte molecules. Mainly they include enzymatic amplification [54], amplification through hybridization chain reaction (HCR) [55,56], rolling circle amplification (RCA) [57,58], and catalytic hairpin assembly (CHA) [55,59,60].

Detection mechanisms in electrochemical aptasensors are mainly based on changes in conductivity (increase or decrease of electron transfer rate) of the signal transducer in the absence/presence of the analyte. When the analyte molecule is present, it captures by the aptamer on the electrode surface, forming an aptamer-target complex that will change the access of redox marker molecules to the surface of the electrode. Aptamers bind to their target biomolecules through hydrogen bonding, electrostatic interactions, hydrophobic interactions, and van der Waals forces [61,62]. As mentioned before, this binding event leads to a change in the electrochemical properties of the electrode surface, which can be measured by various electrochemical techniques, such as voltammetric, amperometry, impedance spectroscopy, electrochemiluminescence (ECL), and photoelectrochemical (PEC) techniques. The change in the electrochemical signal is transduced into a measurable signal, such as a current or voltage, and the magnitude of the signal is proportional to the concentration of the analyte molecule added to the system. Changes in electron transfer rate are always directly related to different concentrations of analytes, which can categorize electrochemical aptasensors into signal-off or signal-on types.

This review covers the most up-to-date (2021–2023) research on the topic in a way that the contents presented here have not been presented completely in previous reviews. In addition, the emphasis on the diagnostic mechanisms in detail and explaining the platforms used for cancer diagnosis are other features presented in this review, which can be a suitable achievement for application in electrochemical biosensors.

Concisely, the design details of the electrochemical aptasensors and elements used in their construction have been schematically presented in Fig. 1. Due to the limited space for the scheme, we could only provide some of the biosensing platforms or elements in this Figure, but the most frequent ones.

2. Electrochemical aptasensors equipped with gold-based nanomaterials for the detection of cancer biomarkers

2.1. Prostate-specific antigen (PSA) electrochemical aptasensor (s) equipped with gold-based nanomaterials

PSA is a glycoprotein found only in the epithelium of the prostate gland. PSA is considered the primary biomarker for the diagnosis of prostate cancer. The normal level of PSA in men is $\leq$ 4 ng mL^{-1} [63]. However, while PSA is a useful biomarker, it is not the only perfect way. PSA can be elevated in other conditions besides prostate cancer, such as benign prostatic hyperplasia and prostatitis. In addition, some men with prostate cancer may have low PSA levels, and some men with elevated PSA levels may not have prostate cancer. As a result, while PSA is a valuable tool for detecting prostate cancer, it is insufficient to diagnose the disease. Other assays, such as a biopsy, may be necessary to confirm the presence of prostate cancer [64,65].

Gold-based nanomaterials have several advantages that make them attractive for a wide range of biosensing applications. These materials are generally biocompatible, chemically stable, and excellent electrically conductive. Moreover, they can be easily synthesized in various sizes and shapes. This versatility allows them to be tailored for specific applications [31].

A PSA aptasensor was developed by applying two aptamer sequences as the biorecognition element [66]. First, GE modified with gold nanoparticles (AuNPs) was prepared as the signal transducer. In the next step, the GE/AuNPs was functionalized with 11-amino-1-undecanothiol to improve the interaction between the AuNPs and the biorecognition element. Then, two thiol-functionalized aptamer sequences specific for the detection of glycosylated and total PSA were immobilized on the surface of electrodes. Finally, various concentrations of analytes were added, and electrochemical assays were monitored by EIS. The designed impedimetric (differences between charge transfer resistance (Rct) values) aptasensing platform could diagnose the cancer biomarker by distinguishing glycosylated and total PSA values. Here, in the presence of analyte concentrations, the Rct values were enhanced, while this reduction in conductivity of the signal transducer was more for glycosylated PSA than the total PSA. This aptasensor could detect the glycosylated and total PSA in ranges from 0.26 to 62.5 ng mL^{-1} (limit of detection (LOD): 0.26 ng mL^{-1}) and from 0.64 to 62.5 ng mL^{-1} (LOD: 0.64 ng mL^{-1}), respectively.

The detection of PSA was monitored by a PEC-based aptasensor [67]. In order to design the aptasensing platform, an ITO electrode modified with a layer of AuNPs was employed as the signal transducer. Then, the surface of this signal transducer was modified with photoactive nanomaterials, including lanthanum titanium oxide ($La_2Ti_2O_7$) and cadmium sulfide/boron sulfide (CdS/b_2S_3), respectively. Afterward, an amine-functionalized capture aptamer sequence and a carboxyl-functionalized aptamer conjugated with vanadium pentoxide (V_2O_5) nanospheres were immobilized on the electrode surface, respectively. In the absence of the analyte, aptamers were in a hybridized (interaction was based on 1-ethyl-3-(-3-dimethylaminopropyl) carbodiimide hydrochloride/N-Hydroxysuccinimide (EDC/NHS) chemistry) status. Finally, various analyte concentrations were added, and measuring was performed by PEC. The detection principle was based on the presence of V_2O_5 nanospheres (here, as a signal quencher). While in the presence of the analyte, the conjugated aptamer with V_2O_5 nanospheres was released from the surface, and the capture aptamer sequence could capture the analyte molecules. So, along with removing V_2O_5 nanospheres from the surface, the PEC signal was enhanced (signal on).

2.2. Carcinoembryonic antigen (CEA) electrochemical aptasensor (s) equipped with gold-based nanomaterials

CEA is a protein normally produced during fetal development, but its production decreases significantly after birth. However, in certain types of cancer, including colorectal, pancreatic, breast, lung, and ovarian cancer, CEA production may increase significantly, leading to elevated levels in the bloodstream [68,69]. The normal level of this biomarker is from 0 to 2.5 ng mL^{-1} [70]. CEA is used as a cancer biomarker, which can also be used to monitor the progress of cancer treatment or to detect cancer recurrence. However, it is important to note that elevated CEA levels can also be caused by non-cancerous conditions such as inflammation, infection, or smoking and that not all people with cancer have elevated CEA levels [71]. Therefore, CEA should be used in combination with other diagnostic tests and clinical assessments to make a definitive cancer diagnosis [72,73].

In a research, CEA detection was followed by an aptasensing platform [74]. Here, a GCE was modified with Au–Pd–Pt-two-dimensional titanium carbide Ti_3C_2Tx nanocomposite and employed as the signal transducer. Then, a mixture of two aptamers was immobilized on the surface. Afterward, two hairpin (HP) structure DNAs were mixed with the analyte. After activating two target amplification cycles, the output DNA was added to the surface of the signal transducer, and DPVs in the presence of hemin/H_2O_2 were recorded. The presence of the analyte led

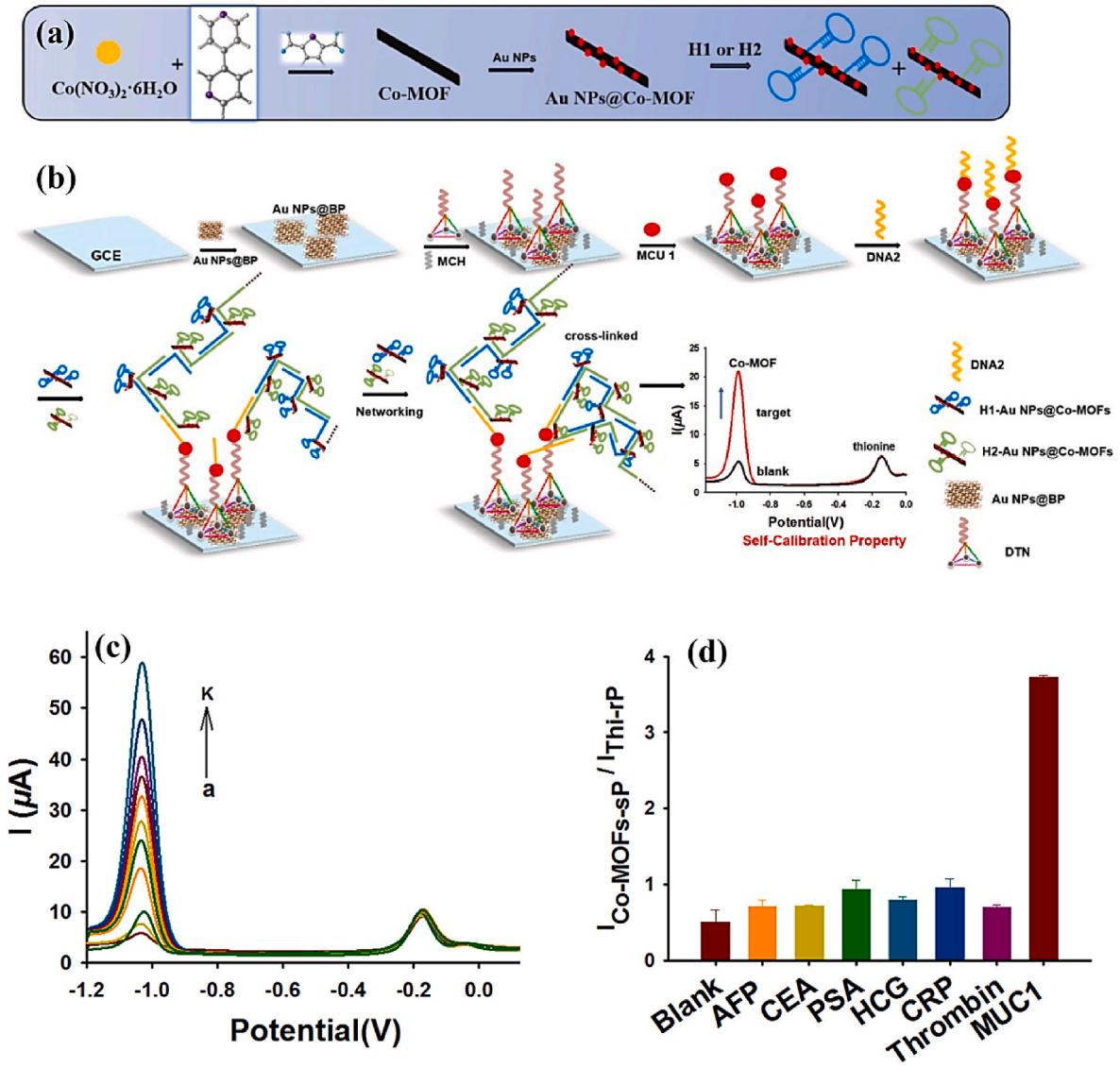

Fig. 2. An electrochemical aptasensing platform designed for detection of CA 15–3; production procedure of Au NPs@Co-MOFs nanocomposite and then conjugation with HP1 and HP2 DNA sequences **(a)**; designing the aptasensing platform on the surface of a GCE **(b)**; DPV behavior against enhancing the concentrations of analyte **(c)**; and the selectivity assay of aptasensor in the presence of several interfering agents **(d)**; License Number: 5427831027617.

to production structures that could carry hemin molecules and electrocatalytic reduction of H_2O_2 mediated by hemin (signal on).

2.3. Mucin-1 (cancer antigen 15–3 (CA 15–3)) electrochemical aptasensor (s) equipped with gold-based nanomaterials

CA 15–3 is a protein expressed on the surface of many cancer cells, including breast, lung, pancreatic, ovarian, and prostate cancers. As such, it is considered a potential cancer biomarker that could be used to support diagnosis or monitor cancer [75,76]. The detection range reported via the enzyme-linked immunosorbent assay (ELISA) for this biomarker is from 0.625 to 40 ng mL^{-1}. CA 15–3 is normally present in the body to protect and lubricate the surfaces of tissues and organs, but in cancer cells, it is often overexpressed in ways that make it more likely to promote cancer growth. Because of this, researchers are interested in developing assays that can detect this biomarker in blood, urine, or other bodily fluids to identify the presence or progression of cancer [77].

In a research, an aptasensor was designed to detect CA 15–3 as a cancer biomarker [78]. Initially, Au NPs@Co-Metal-organic frameworks (MOFs) nanocomposite was synthesized from a mixture solution of Au NPs (produced from $HAuCl_4$ and trisodium citrate) and Co-MOF (produced from $Co(NO_3)_2{\cdot}6H_2O$, dimethylformamide (DMF), 2,5-Thiophenedicarboxylic acid, and 4,4′-bipyridine (Bpy)) (Fig. 2). Since the mentioned nanocomposite contained the carboxyl functional group, the EDC/NHS was applied for activation. Afterward, streptavidin (SA) and two biotin-functionalized hairpin DNA sequences (HP1 and HP2) were added and conjugated with the nanocomposite (HP1/HP2–Au NPs@Co-MOFs). On the other hand, a GCE was utilized as the signal transducer, which was physically modified with Au NPs@black phosphorus (BP) nanocomposite. Subsequently, DNA nanotetrahedrons (DTN), as a part of the biorecognition element, were immobilized on the surface of the electrode. Three sequences of the DTN were thiol-functionalized and could create the Au–S bond with Au NPs@BP nanocomposite on the surface of the electrode. Then, the various concentrations of analyte were added, which were captured by one DNA sequence related to the DTN (CA 15–3 aptamer) from one side. Then another DNA sequence (DNA2) was added, captured the analyte from the other side, and completed a sandwich-like structure (Fig. 2). Finally, the HP1/HP2-AuNPs@Co-MOFs structure was added and interacted with DNA2. The presence of the analyte was necessary for attachment of

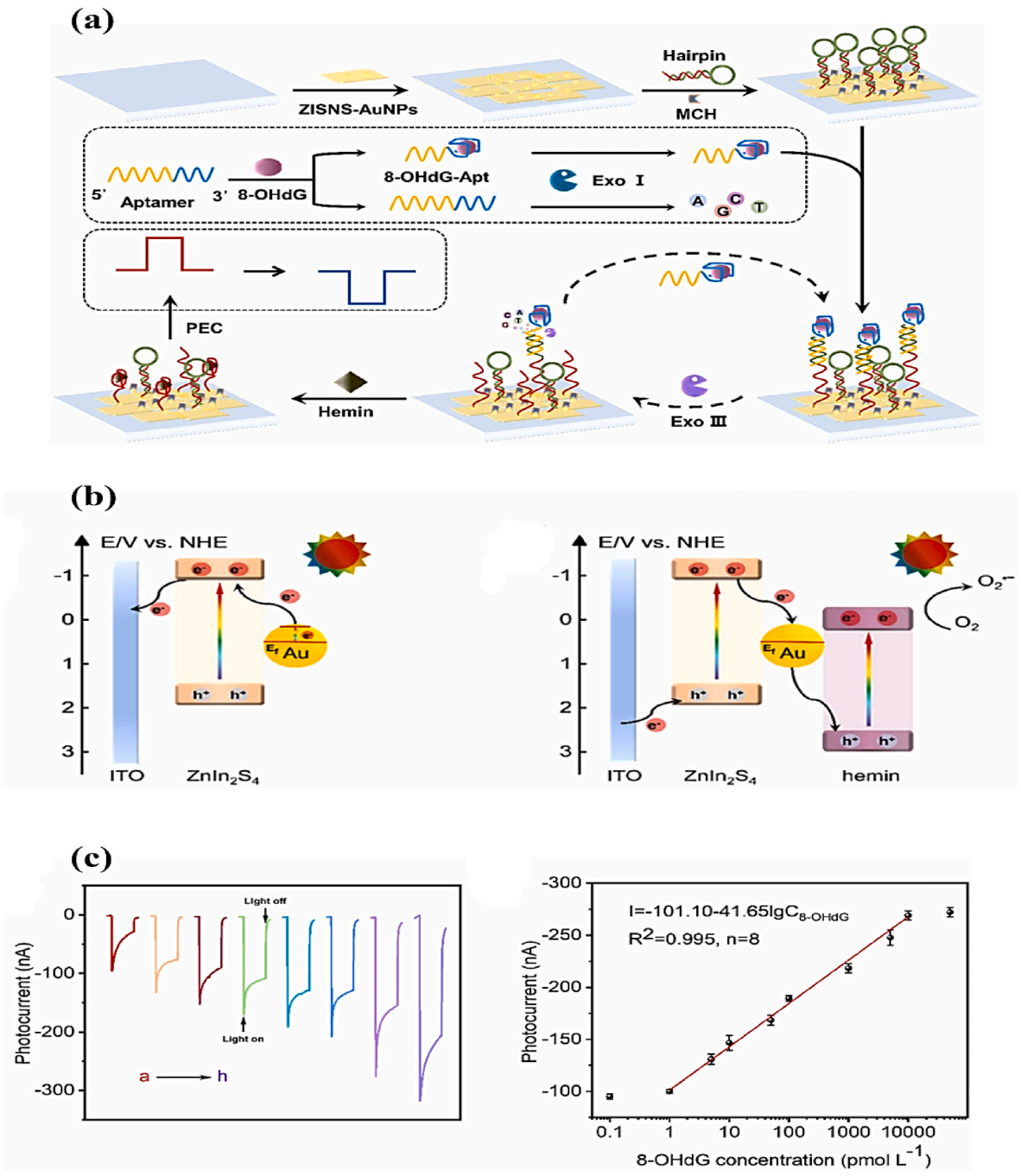

Fig. 3. An aptasensing platform designed for detection of 8-OHdG; various steps for assembly of aptasensor on the surface of an ITO electrode **(a)**; mechanism of detection in the absence/presence of the analyte directed by AuNPs-$ZnIn_2S_4$ nanohybrids **(b)**; PEC signals and calibration curve related to various concentrations of the analyte **(c)**; License Number: 5430260369739.

HP1/HP2-AuNPs@Co-MOFs structure on the electrode surface where this structure activated a HCR signal amplification process, and the presence of AuNPs@Co-MOFs nanocomposite was causing for enhancing the DPV peak currents (signal-on). This aptasensor detected CA 15–3 in a range from 0.004 to 400 pM, and the obtained LOD was 1.34 fM.

In another research, the detection of CA 15–3 was followed by another aptasensor assembly [79]. Here, an amine-functionalized DNA sequence (HP1) was immobilized on the surface of a GCE modified with AuNPs. Then, the analyte and another aptamer sequence were mixed and added to a solution containing AuNPs@Cu_7S_4@Cu/Mn-azo-based porous organic polymer (AzoPPOP)-HP2. This biosensor was equipped with two signal amplification agents: CHA and inorganic-organic polymer hybrid mimic peroxidase (AuNPs@Cu_7S_4@Cu/Mn-AzoPPOP) nanocomposite. The electrochemical detections were followed by chronoamperometry (CA) and DPV techniques (signal-on). The linear detection range for this aptasensor was from 1 fg mL^{-1} to 10 pg mL^{-1}.

The detection of CA 15–3 was shadowed by an aptasensor designed by using two electrochemical assays (DPV and CA) [80]. Here, a GCE was used as the working electrode and modified with AgNPs through an electrodeposition method. Then a thiol-functionalized aptamer was added to the surface and established the Ag–S bond. Unwanted and non-specific aptamer binding sites were blocked by 6-mercapto-1-hexanol (MCH). Afterward, the analyte was added and captured by aptamer

strands from one side. Consequently, MnO@C@AuNPs nanocomposite was produced and conjugated with the thiol-functionalized aptamer strands and could create covalent interaction with AuNPs. This structure was added to the surface of the electrode and captured the analyte from the other side by developing a sandwich-like structure. This aptasensor used two electrochemical detection techniques to measure the analyte's various concentrations. The detection mechanism was based on the redox behavior of the MnII/MnIV couple and H_2O_2 induced to the aptasensing platform. By increasing the analyte concentration, the currents for both assay techniques amplified and introduced a signal-on aptasensor for CA 15–3. The presented aptasensor could detect the analyte in ranges from 0.001 to 100 nM (LOD: 0.31 pM) and 0.001–10 nM (LOD: 0.25 pM) for DPV and CA, respectively.

2.4. 8-Hydroxy-2′-deoxyguanosine (8-OHdG) electrochemical aptasensor (s) equipped with gold-based nanomaterials

8-OHdG is a biomarker that is used to assess oxidative damage to DNA in cells. It is a modified form of the DNA base guanine, which can occur due to exposure to reactive oxygen species (ROS) that are generated as byproducts of cellular metabolism or as a result of exposure to environmental toxins, radiation, or other sources of oxidative stress. Elevated levels of 8-OHdG have been detected in various cancers, including lung, breast, liver, and bladder cancer. The reported normal level of 8-OHdG in males and females is 29.6 ng mg $^{-1}$ and 43.9 ng mg $^{-1}$, respectively [81]. The presence of 8-OHdG in urine or other bodily fluids can thus serve as a potential biomarker for the early detection of these cancers or for monitoring the effectiveness of treatment. However, it is important to note that elevated levels of 8-OHdG can also occur due to other factors, such as inflammation or infection. Thus the use of this biomarker for cancer detection or monitoring may not be specific to cancer only [82,83].

In a research, 8-OHdG as a cancer biomarker was detected by a PEC aptasensor using a modified ITO electrode with AuNPs-$ZnIn_2S_4$ nanohybrids [84]. In order to design the sensing platform, an ITO electrode was used as the signal transducer, which was modified with AuNPs-$ZnIn_2S_4$ nanohybrids through the drop-casting procedure. The presence of this nanomaterial improved the surface performance and acted as a signal amplifier. Then, a thiol-functionalized HP aptamer was immobilized on the surface and interacted with gold through the Au–S covalent bond. Subsequently, the unwanted aptamer strands were blocked by MCH (Fig. 3). Afterward, various concentrations of analyte were added and incubated on the surface with the aptamer strands, and unbound aptamer strands with the analyte were eliminated by exonuclease I. In the next step, exonuclease III and hemin-G-quadruplex nanostructure (aimed at polarity switching on the surface of the signal transducer) were added, respectively. The presence of exonuclease III was the reason for opening the hairpin structure of aptamer strands and releasing aptamer-analyte couple in a cycle, which via adding the hemin to the system, led to the reversal of photocurrent polarity (Fig. 3). The performance of this aptasensor for detecting analyte was in a linear range from 1 pM to 10 nM and with a LOD of about 0.3 pM.

2.5. Epithelial cell adhesion molecule (EpCAM) electrochemical aptasensor (s) equipped with gold-based nanomaterials

EpCAM is a transmembrane glycoprotein which considered as a cancer biomarker expressed on the surface of most normal and malignant epithelial cells [85]. EpCAM is overexpressed in many types of cancer, including breast, colon, lung, prostate, ovarian, and pancreatic cancers [86]. EpCAM assays have been developed in preclinical and clinical studies for the diagnosis and prognosis of cancer. Measuring the levels of EpCAM in the patient's blood or tissue samples can provide useful information for improving cancer diagnosis and treatment. In healthy individuals, EpCAM expression can vary depending on the tissue or organ being examined, but generally, it is expressed at low levels [87]. However, in cancer, EpCAM expression can be upregulated, and its levels may be significantly higher compared to normal tissues. The level of EpCAM expression can vary depending on the type and stage of cancer. Some cancers, such as breast cancer and ovarian cancer, often exhibit high levels of EpCAM expression [88,89]. In contrast, other types of cancer, such as leukemia and lymphoma, typically do not express EpCAM or express it at low levels [90]. EpCAM assay is particularly useful for detecting circulating tumor cells (CTCs) in the blood of cancer patients, which can help predict treatment response and disease progression [91,92].

An aptasensing platform was developed for the detection of EpCAM [93]. A magnetic glassy carbon electrode (MGCE) was used as the signal transducer and modified with Co-MOF-Fe_3O_4 and Ag nanosheets (NSs), respectively. Afterward, a thiol-functionalized complementary DNA sequence was immobilized on the surface. Subsequently, EpCAM-aptamer conjugated with AuPt NPs was added to the surface and hybridized with the complementary DNA. In the presence of the analyte, the hybridized structure was cleaved, EpCAM-aptamer conjugated with AuPt NPs released, and then it captured the analyte molecules. So, in the presence of the analyte, since many AuPt NPs were removed from the direct connection to the surface of the signal transducer, the peak current of DPVs was reduced (signal off).

In another research, the detection of EpCAM-positive cancer cells was followed by an aptasensor [94]. A SPE was applied as the signal transducer and modified with SiNPs and Au nanostars, respectively. Then, a thiol-functionalized aptamer sequence was immobilized on the surface and interacted with the gold surface. Afterward, cancer cells (analyte) were added and captured by aptamer strands from one side. At the next step, a cholesterol-labeled DNA probe was added to the surface of the signal transducer. It could capture the analyte from another side (through binding to the membrane of cancer cells via hydrophobic interactions). This probe was equipped with phi29 DNA polymerase and could activate the RCA that catalyzed the redox reaction of tris (2-carboxyethyl) phosphine, 3, 3′, 5, 5′-tetramethylbenzidine dihydrochloride. This biosensing platform was equipped with dual signal amplification (application of nanomaterials and the RCA) process and used DPV for electrochemical measurements (signal-on).

2.6. Interferon-γ (IFN-γ) electrochemical aptasensor (s) equipped with gold-based nanomaterials

IFN-γ is a cytokine that plays an important role in the immune system's response to cancer. It is produced by activated T cells, natural killer cells, and other immune cells, and it has been shown to have both antitumor and protumor effects depending on the context [95]. As a biomarker for cancer, IFN-γ has been studied in various cancers and has shown promise as a prognostic biomarker. In one study, this biomarker's normal range was reported from 0.1 to 2 pg mL^{-1} [96]. In some studies, elevated levels of IFN-γ have been associated with a better prognosis in certain types of cancer, including breast, ovarian, and colorectal cancers [97]. In these cases, IFN-γ is thought to stimulate an immune response against the cancer cells and help to control tumor growth. On the other hand, in other types of cancer, such as melanoma and lung cancer, IFN-γ has been shown to promote tumor growth and resistance to immunotherapy [98]. In these cases, elevated levels of IFN-γ may be indicative of a more aggressive cancer that is less responsive to treatment. Overall, the role of IFN-γ as a biomarker for cancer is complex and context-dependent [99,100].

In a research, an electrochemical aptasensor was developed to detect IFN-γ using an amine-functionalized GCE as the working electrode [101]. Here, the surface of the mentioned signal transducer was treated with an amino group in a photochemical reaction. Then, the surface of the electrode was modified with AuNPs by immersing it in an acidic solution of gold. Afterward, a thiol-functionalized aptamer was immobilized on the surface, interacted with gold strongly, and produced GCE/AuNPs/aptamer. After blocking unwanted aptamer strands by

Table 1
Main elements used in electrochemical aptasensors equipped with gold-based nanomaterials for the detection of cancer biomarker.

Analyte	Signal transducer	Aptamer and/or oligonucleotide sequence (s)	Aptamer functional group	Nanomaterial (s)	Detection technique (s)	Real sample	Detection range	LOD	Ref.
PSA	GE	5′-AATTAAAGCTCGCCATCAAATAGCTTT-3’/5′-GAGCGGGGTTGCT GGGATGATAAGGCCCCTTTGATGTCTG-3′	Thiol	AuNPs	EIS	Serum	0.26–62.5 ng mL^{-1}/ 0.64–62.5 ng mL^{-1}	0.26 ng mL^{-1}/ 0.64 ng mL^{-1}	[66]
PSA	GCE	5′-ATTAAAGCTCGCCATCAAATAGC-3’/ 5′-ATTAAAGCTCGCCATCAAATAG-3’/5′-ATTAAAGCTCGCCATCAAATAGC-3′	Amine/ Thiol	MoS_2nanoflowers/Au nanobipyramids	PEC	Serum	0.005–100 ng mL^{-1}	0.39 pg mL^{-1}	[102]
PSA	GCE	5′-TTTTTAATTAAAGCTCGCCATCAAATAGCTTT-3′	Amine	AuNPs@Co phthalocyanine nanocomposite	EIS/DPV	Serum	1.2–2 pM	0.025 ng mL^{-1}	[103]
PSA	ITO	5′-GCTATTTGACAGCTTTAAT-3’/5′- ATTAAAGCTCGCCATCAAATAGC-3′	Amine/ Carboxyl	AuNPs/$La_2Ti_2O_7$nanosheets/ V_2O_5 nanosphere/	PEC	Serum	1×10^{-5} - 500 ng mL^{-1}	4.3 fg mL^{-1}	[67]
CEA	GE	5′-ACGCACCAGACACCACGACA-3′	Thiol	AuNPs	SWV	Serum	1 pg mL^{-1} - 100 ng mL^{-1}	0.479 pg mL^{-1}	[104]
CEA	GE	5′- CGTGTATGCGTTGCACAATTTTTTTTTTAATTGAATAAGCCGCATACA CG-3’/5′-ATACCAGCTTATTCAATT-3′	Thiol	AuNPs	SWV	Serum	10 pg mL^{-1} - 100 ng mL^{-1}	1.9 pg mL^{-1}	[105]
CEA	GCE	Several aptamer and/or oligonucleotide sequences applied in detection and target amplification	Thiol	Au–Pd–Pt–Ti_3C_2Tx nanocomposite	DPV	Serum	1 fg mL^{-1} - 1 ng mL^{-1}	0.32 fg mL^{-1}	[74]
CEA	GCE	5′-AGGGGGAAGGGATACCC-3′	Thiol	CdS quantum dots (QDs) @MOF nanocomposite/ Triethanolamine@AuNPs nanocomposite	ECL	Serum	0.0001–10 ng mL^{-1}	8.5×10^{-5} ng mL^{-1}	[106]
CA 15-3	GCE	5′-TCGTGTGGCCAGGGTATCCAGCTGAGCAGTTGATCCTTTGGATACCCTGG-3′	—[a]	Inorganic-organic polymer hybrid mimic peroxidase (AuNPs@Cu_7S_4@Cu–Mn-AzoPPOP) nanocomposite	DPV/CA	Serum	1 fg mL^{-1} - 10 pg mL^{-1}	DPV: 0.72 fg mL^{-1}/ CA: 0.82 fg mL^{-1}	[79]
CA 15-3	GCE	Several aptamer and/or oligonucleotide sequences applied in detection and target amplification	Thiol/ Biotin	DTN/AuNPs@BP nanocomposite/Au NPs@Co-MOF nanocomposite	DPV	Serum	0.004–400 pM	1.34 fM	[78]
CA 15-3	GCE	Several aptamer and/or oligonucleotide sequences applied in detection and target amplification	Thiol/ Biotin	Au NPs-MXene nanocomposite/Au NPs-UiO-66-NH_2 MOFs nanocomposite/ Magnetic beads	DPV	Serum	5 pg mL^{-1} - 50 ng mL^{-1}	0.72 pg mL^{-1}	[107]
CA 15-3	GCE	5′- GCAGTTGATCCTTTGGATACCCTGG-3’/5′- TTTCCAGGGTATCCAAAGGA TCAACTGC-3′	Thiol	AuNPs	SWV	Artificial serum	0.1–200 pM	0.087 pM	[108]
Circulating tumor cells (CTCs)	SPE	5′- TGAAGGTTCGTTGTTTCGGTGGGTGTAGACTCTTTAGAAGAGATACAGA TTTTGGGAATG-3′	Thiol	SiNPs/Au nanostars	DPV	Serum	5 - 10^7 cells mL^{-1}	1 cells mL^{-1}	[94]
CTCs	Paper based electrode	5′-GCAGTTGATCCTTTGGATACCCTGG-3′	Thiol	AuNPs	DPV	MCF-7 cells in serum	20–1 × 10^6 cell mL^{-1}	7 cell mL^{-1}	[109]
CTCs	GCE	5′-TGCAGTTGATCCTTTGGATACCCTGGT-3′	Biotin	AuNPs	DPV	MCF-7 breast cancer cell line	5×10^2–1.5 × 10^5 cells mL^{-1}	50 cells	[110]
CTCs	GCE	5′- CCCCCCCACTACAGAGGTTGCGTCTGTCCCACGTTGTCATGGGGGGT TGGCCTG-3′	Thiol	Highly fractal Au nanostructures/2D Au@PdMo nanocomposite	DPV	Serum	2–1 × 10^5 cells mL^{-1}	2 cells mL^{-1}	[111]
Prostatic CTCs	Screen-printed gold electrode (SPGE)	5′-GGAGGACGAUGCGGAUCAGCCAUGUUUACGUCACUCUUCUACCUCGUCHUCU UUUUUACGUCACUCU-3′	Thiol	AuNPs	EIS	—[b]	1 - 40 cells mL^{-1}	0.62 cells mL^{-1}	[112]
Tumorous exosomes	GE	5′- CACCCCACCTCGCTCCCGTGACACTAATGCTA-3′	–	AuNPs	DPV	Plasma	500 - 5000 particles μL^{-1}	482 particles μL^{-1}	[113]

(*continued on next page*)

Table 1 (*continued*)

Analyte	Signal transducer	Aptamer and/or oligonucleotide sequence (s)	Aptamer functional group	Nanomaterial (s)	Detection technique (s)	Real sample	Detection range	LOD	Ref.
IFN-γ	GCE	5′-GGGGTTGGTTGTGTTGGGTGTTGTGTCCCCTCAATCCC-3’/5′-ACACAACACCCAA CACAACCAACCCC-3′	Thiol	AgNCs/AuNPs	LSV	Serum	5–1000 pg mL^{-1}	1.7 pg mL^{-1}	[101]
EpCAM	GCE	5′- CACTACAGAGGTTGCGTCTGTCCCACGTTGTCATGGGGGGTTGGCCTG-3’/5′- GA CGCAACCTCTGTAGTG-3′	Thiol	Au–Pt nanocomposite/Co-MOF-Fe_3O_4–Ag NSs nanocomposite	DPV	Serum	100 pg mL^{-1}- 100 ng mL^{-1}	13.8 pg mL^{-1}	[93]
Cancer antigen 125 (CA-125)	GCE	5′- ACCACCACCACGACGCACGAGTACCCCGCG-3′	Thiol	AuNPs	DPV	Serum	0.1–1000 U mL^{-1}	0.027 U mL^{-1}	[114]
Vascular endothelial growth factor (VEGF) 165	GE	5′-TTTTTTTTGTGGGGGTGGACGGGCCGGGTAGA-3’/5′-TTTTTTTTTTTTTTTTTTTTCAATTGGGCCCGTCCGTATGGTGGGT-3′	Thiol	AuNPs	DPV	Whole Blood	1 pg mL^{-1} - 10 ng mL^{-1}	0.67 pg mL^{-1}	[115]
VEGF165	GCE	Several aptamer and/or oligonucleotide sequences applied in detection and target amplification	Thiol/ Biotin	AuNPs	ECL	Serum	0.5 pg mL^{-1} - 500 ng mL^{-1}	0.2 fg mL^{-1}	[116]
VEGF165	MGCE	5′-CAATTGGGCCCGTCCGTATGGTGGGT-3′	Thiol	Fe_3O_4–Fe_2O_3@AuNPs nanocomposite	DPV	Serum	0.01–10 pg mL^{-1}	0.01 pg mL^{-1}	[117]
Thrombin	GCE	Several aptamer and/or oligonucleotide sequences applied in detection and target a mplification	Thiol	AuNPs-$Ti_3C_2T_x$nanocomposite	Alternating current voltammetry (ACV)	Serum	5 fM- 1 pM	1.7 fM	[118]
8-OHdG	ITO	5′-GGGTTGGGCGGGATGGGTTACCTCAGTGCTTATTCAACCCTATTA-3’/5′-TAATAGGGTTGAATAAGCACTGAGGTGCGGGCGATCGGCGGGGGGTGCGTGCGCTCT GTGCCAGGGGGTGGGACAGA TCATATGGGGGTGCT-3′	Thiol	AuNPs	PEC	Serum	1.0 pM - 10 nM	0.3 pM	[84]
Leptin	SPE	5′- GTTAATGGGGGATCTCGCGGCCGTTCTTGTTGCTTATACA-3’/3′-CAATTACCCCCTAGAGCGCCGGCAAGAACAACGAATATGT-5′	Thiol/ Biotin	ZnONPs/AuNPs	DPV	Serum/ Plasma	0.01–100 pg mL^{-1}	0.0035 pg mL^{-1}	[119]
MCF-7 breast cancer cells	GCE	Several aptamer and/or oligonucleotide sequences applied in detection and target amplification	Biotin/ Thiol	AuNPs/VS_2NSs	DPV	Whole blood	10–1 × 10^5 cells mL^{-1}	5 cells mL^{-1}	[120]
MCF-7 breast cancer cells	ITO	5′-GCAGTTGATCCTTTGGATACCCTGG-3′	Thiol	AuNPs-Bi_2O_2S nanocomposite	PEC	Serum	50–6 × 10^5 cell mL^{-1}	17 cell mL^{-1}	[121]
Proteoglycan 3	GCE	5′- TAACGCTGACCTTAGCTGCATGGCTTT ACATGTTCCA-3’/5′-TAACGCTGACCTTAGCTGCATGGCTTTACATGTTCCA-3′	Thiol	Nd-MOF@AuNPs nanocomposite	PEC	Serum	0.001–10 ng mL^{-1}	0.66 pg mL^{-1}	[122]
Human epididymis protein 4 (HE4), an ovarian cancer tumor biomarker	MGCE	5′-TTATCGTACGACAGTCATCCTACAC-3’/5′-TTTTTTTTTTTTTGTCGTACGAT-3′	Thiol	Fe_3O_4-α-Fe_2O_3@Au nanocomposite	DPV	Serum	0.1 pg mL^{-1} - 1 ng mL^{-1}	27.5 fg mL^{-1}	[123]
Human apolipoprotein A-I (ApoA1)	GCE	5′-CCTCGGCACGTTCTCAGTAGCGCTCGCTGGTCATCCCACA-3′	Thiol	Gold nanorods (Au NRs)- gold nanowires nanocomposite	DPV	Serum	0.1–1000 pg mL^{-1}	0.04 pg mL^{-1}	[124]

[a] Functional group of aptamer and/or oligonucleotide sequence (s) not reported.
[b] Real sample application not reported.

MCH, various concentrations of the analyte were added to the surface. Subsequently, a complementary DNA sequence was added and hybridized with the aptamer sequence. Finally, the duplex-specific nuclease was used to cleavage the hybridized form of the DNA/aptamer, and by adding $AgNO_3$ and $NaBH_4$, a redox reaction processed and led to the production of the silver nanoclusters (AgNCs) as the signal probe on the surface of the electrode which created the electrochemical signal. In the presence of the analyte, peak currents related to the silver oxidation increased by enhancing the concentration of the analyte. The results were followed via the linear sweep voltammetry (LSV) technique and confirmed a signal-on behavior. This aptasensor could detect the analyte in a linear range from 5 to 1000 pg mL^{-1} and with a LOD equal to 1.7 pg mL^{-1}.

Table 1 presents the critical features of electrochemical aptasensors designed to detect cancer biomarkers equipped with gold-based nanomaterials. Classifications were mainly based on the type of cancer analyte, signal transducer, and other vital features.

3. Electrochemical aptasensors equipped with carbon-based nanomaterials for the detection of cancer biomarkers

3.1. CA 15–3 electrochemical aptasensor (s) equipped with carbon-based nanomaterials

In a research, the detection of CA 15–3 was followed by an aptasensor developed for two electrochemical detection techniques [125]. A GCE modified with hemin-graphene@PdPtNPs nanocomposite was applied as the signal transducer. In the next step, the CA 15–3 aptamer was mixed with an amine-functionalized complementary DNA, and a desired amount of the hybridized structure was added to the electrode surface. Then, the various analyte concentrations were added, and then electrochemical measurements were followed by DPV and CA techniques. In the absence of the analyte, the hybridized structure on the surface acted as a hindering agent for electron transfer related to hemin. In contrast, the presence of the analyte led to releasing the complementary DNA from the surface, and aptamer strands could capture analyte molecules. In this condition, the access for hemin molecules to the surface of the signal transducer was increased, and electrochemical signals were amplified (signal on).

3.2. CEA electrochemical aptasensor (s) equipped with carbon-based nanomaterials

In a research, a GE was used as the signal transducer and then treated with a thiol-functionalized aptamer (Apt1) and analyte, respectively. Afterward, the conjugated form of another aptamer sequence (Apt2) and poly (ferrocenyl glycidyl ether)-grafted single-walled carbon nanotubes (PFcGE-SWCNTs) was added to the surface, and the analyte was placed in a sandwich like status. The electrochemical measurements of CEA were followed by SWV, and the results confirmed a signal-on biosensor due to the presence of the PFcGE-SWCNTs nanocomposite as a signal amplifier [126].

3.3. Multiplexed electrochemical aptasensor (s) equipped with carbon-based nanomaterials

A multiplexed aptasensor has been introduced for the simultaneous detection of three cytokines (VEGF, IFN-γ, and tumor necrosis factor-alpha (TNF-α) [127]. Here, a GE modified with a mixture of graphene oxide (GO)/SA was utilized as the signal transducer. Then, biotin-functionalized aptamers related to analytes were added; each aptamer was labeled with a different redox marker where anthraquinone (AQ), methylene blue (MB), and ferrocene (Fc) were used for VEGF, IFN-γ, and TNF-α aptamers, respectively. Then, the desired concentrations of analytes were added, and the electrochemical biosensing was shadowed by SWV. The presence of analytes changed the conformation of aptamers, which changed the position of redox marker molecules at a far distance from the surface of the electrode. This event decreased the SWV peak currents (signal-off).

Table 2 presents the critical features of electrochemical aptasensors designed to detect cancer biomarkers equipped with carbon-based nanomaterials. Classifications were mainly based on the type of cancer analyte, signal transducer, and other vital features.

4. Electrochemical aptasensors equipped with gold/carbon-based nanomaterials for the detection of cancer biomarkers

4.1. Acute lymphoblastic leukemia (ALL) electrochemical aptasensor (s) equipped with gold/carbon-based nanomaterials

CCRF-CEM is a cell line derived from human ALL cells commonly used as a model system for studying leukemia and cancer biology. Research using the CCRF-CEM cell line has provided insights into the molecular mechanisms of leukemia development and progression, as well as the mechanisms of action of chemotherapeutic agents [150]. The CCRF-CEM cell line has also been used to screen potential anti-leukemia drugs and to develop new therapeutic strategies for ALL. As such, the normal range for CCRF-CEM cells is not applicable as they are derived from cancerous cells [150].

An aptasensor has been introduced to diagnose the ALL by applying a graphite SPE modified with Au-graphene nanocomposite as the signal transducer [151]. A thiol-functionalized aptamer was immobilized on the surface of the nanoelectrode and interacted with gold agents through the Au–S covalent bond. Then, the analyte was added, and a conjugated structure containing a copper sulfide-graphene (CuS-GR) nanocomposite and an aptamer was added. So, the analyte was located in a sandwich-like state between aptamer strands. The analysis was performed by DPV, and this aptasensor showed a signal-on behavior for detecting CCRF-CEM cancer cells. The signal-on behavior was due to the presence of CuS-GR nanocomposite as one part of the biosensing platform that facilitated the redox reactions.

4.2. Tumor exosomes electrochemical aptasensor (s) equipped with gold/carbon nanomaterials

Tumor exosomes are small (40–180 nm in diameter) extracellular vesicles that are secreted by cancer cells [152]. They are released by cells into the extracellular space and can be found in various bodily fluids, including blood, urine, and saliva. Tumor exosomes contain a variety of biomolecules, including proteins, lipids, and nucleic acids. They play a crucial role in intercellular communication and can affect the behavior of recipient cells by transferring their contents. Tumor exosomes have been shown to promote tumor growth and metastasis and are being studied as potential biomarkers for cancer diagnosis and prognosis [153,154].

Another aptasensor was developed to detect tumor exosomes related to breast cancer MCF-7 cells [155]. In this aptasensor, a GCE was used as the signal transducer and modified with chitosan (CS) and porous nano-carbon, respectively. Then, an amine-functionalized DNA sequence (S-DNA) was immobilized on the surface and could create interaction with porous nano-carbon molecules. At the next step, a hairpin structure MB-labeled DNA sequence (H-MB) was immobilized on the surface and created a strong DPV signal in the absence of the analyte. While, when a mixture of several DNA sequences (cholesterol-probe, aptamer probe (conjugated with Au NPs), and track DNA) and tumorous exosomes related to breast cancer MCF-7 cells were added, the hairpin structure of H-MB opened by an exonuclease and the hybridization positions changed and MB molecules were located in a more far distance from the surface of the signal transducer. Consequently, the DPVs' peak currents decreased (signal-off).

Table 2
Main elements used in electrochemical aptasensors equipped with carbon-based nanomaterials for the detection of cancer biomarkers.

Analyte	Signal transducer	Aptamer and/or oligonucleotide sequence (s)	Aptamer functional group	Nanomaterial (s)	Detection technique (s)	Real sample	Detection range	LOD	Ref.
PSA	GCE	5′- TTTTTAATTAAAGCTCGCCATCAAATAGCTTT-3′	Amine	Graphitic-carbon nitride (gCN) QDs nanocomposite	EIS	Serum	1.2–2 pM	1.2 pM	[128]
PSA	GCE	5′- TTTTTAATTAAAGCTCGCCATCAAATAGCTTT-3′	Amine	Graphene QDs/Nitrogen doped graphene (NG) QDs nanocomposite/GCN QDs nanocomposite	EIS	Serum	GCE-GQDs: 0.034–0.057 ng mL^{-1}/GCE-NGQDs: 0.034–0.057 ng mL^{-1}/ GCE-gCNQDs: 0.034–0.057 ng mL^{-1}	GCE-GQDs: 0.097 ng mL^{-1}/GCE-NGQD: 0.044 ng mL^{-1}/ GCE-gCNQDs: 0.330 ng mL^{-1}	[129]
PSA	GCE	5′-TTTTTAATTAAAGCTCGCCATCAAATAGCTTT-3′	Amine	Graphene QDs	DPV	—[a]	1.2–2 pM	0.66 pM	[130]
CEA	GE	5′-ATACCAGCTTATTCAATT-3’/5′-AGGGGGTGAAG GGATACCC-3′	Thiol	SWCNTs	SWV	Serum	1×10^{-15} - 1×10^{-8} g mL^{-1}	0.28 fg mL^{-1}	[126]
CEA	GCE	5′-ATACCAGCTTATTCAATT-3’/5′-AGGGGGTGAAG GGATACCC-3′	—[b]	Polydopamine functional graphene (PDA@Gr) nanocomposite/Pd–Pt nanocomposite	DPV	Serum	50 pg mL^{-1} - 1 μg mL^{-1}	6.3 pg mL^{-1}	[131]
CEA	Screen-printed carbon electrode (SPCE)	5′-ATACCAGCTTATTCAATT-3′	Amine	Carbon nanotube-decorated MXene NSs nanocomposite	DPV	Serum	10–1×10^{6} pg mL^{-1}	2.88 pg mL^{-1}	[132]
CEA	Interdigitated electrode	3′-TTAACTTATTCGACCTAT-5’/3′-CCCATAGGG AAGTGGGGGA-5′	Amine	Graphene	—[c]	Serum	0.5–500 ng mL^{-1}	0.5 ng mL^{-1}	[133]
Human epidermal growth factor receptor 2 (HER2)	Graphite electrode	5′- GGGCCGTCGAACACGAGCATGGTGCGTGGA CCTAGGATGACCTGAGTACTGTCC-3′	Amine	Reduced graphene oxide (rGO) NSs/Rhodium nanoparticles (Rh NPs)	DPV	–	5–10×10^{4} cells mL^{-1}	3 cells mL^{-1}	[134]
HER2	Graphite electrode	5′- GGGCCGTCGAACACGAGCATGGTGCGTGGA CCTAGGATGACCTGAGTACTGTCC-3′	Amine	rGO NSs/Rh NPs	DPV	Serum	10–500 ng mL^{-1}	0.665 ng mL^{-1}	[135]
HER2	Graphite electrode	5′-GGGCCGTCGAACACGAGCATGGTGCGTGGA CCTAGGATGACCTGAGTACTGTCC-3′	Amine	GO	DPV	Serum	0.5–25 ng mL^{-1}	0.59 ng mL^{-1}	[136]
HER2	GCE	5′-AACCGCCCAAATCCCTAAGAGTCTGCACTTGTCAT TTTGTATATGTATTTGGTTTTTGGCTCTCACAGACAC ACTACACACGCACA-3′	–	Sulphur-nitrogen doped graphene QDs nanocomposite	EIS	Serum	1–10 ng mL^{-1}	0.00141 ng mL^{-1}	[137]
CA 15-3	GCE	5′-GCAGTTGATCCTTTGGATACCCTG G-3’/5′- CGTC AACTAGGAAACCTATGGGACC-3′	Amine	Hemin-graphene@PdPtNPs nanocomposite	DPV/CA	Serum	DPV: 8 pg mL^{-1} - 80 ng mL^{-1}/CA: 0.8 pg mL^{-1} - 80 ng mL^{-1}	DPV: 2.5 pg mL^{-1}/CA: 0.25 pg mL^{-1}	[125]
CA 15-3	3D pen-printed electrode	5′-GCAGTTGATCCTTTGGATACCCTGG-3′	–	Nanocarbon	DPV	MCF-7 breast cancer cell line	20–1000 nM	20 nM	[138]
VEGF	SPCE	5′-AUGCAGUUUGAG AAGUCGCGCAU-3′	Amine	Polyaniline (PANI)-carbon nanotube nanocomposite	DPV	–	0.5 pg mL^{-1} - 1 μg mL^{-1}	0.4 pg mL^{-1}	[139]
VEGF/IFN-γ/TNF-α	GE	VEGF: 5′- AAAAAAAAAACCGTCTTCCAGACAAGAGTGCAGGGAAT CTGGAAGAC-3’/IFN-γ: 5′-TTTTTTTTTTGGGGTTGGTTGTGTTGGGT GTTGTGTCCAACCCC-3’/TNF-α: 5′- TGAGGGTTGTCGCCTGGTGGAT GGCGCAGTCGGCGACAA-3′	Biotin/ Amine	GO	SWV	Serum	VEGF: 5–300 pg mL^{-1}/IFN-γ: 5–300 pg mL^{-1}/ TNF-α: 5–200 pg mL^{-1}	5 pg mL^{-1}	[127]
CA-125	GCE	5′-CTCACTATAGGGAGACAAGAATAAACGCTCAA-3′	Amine	Nickel hexacyanoferrate nanocubes/PDA@Gr nanocomposite	DPV	Serum	0.10 pg mL^{-1} - 1 μg mL^{-1}	0.076 pg mL^{-1}	[140]

(*continued on next page*)

Table 2 (*continued*)

Analyte	Signal transducer	Aptamer and/or oligonucleotide sequence (s)	Aptamer functional group	Nanomaterial (s)	Detection technique (s)	Real sample	Detection range	LOD	Ref.
CA-125	GE	5′-TAATACGACTCACTATAGGGAGACAAGAATAAACGCTCAA-3′	Thiol	G–C_3N_4–Fe_3O_4-PANI nanocomposite	SWV	Serum	5–60 U mL^{-1}	0.298 U mL^{-1}	[141]
Platelet-derived growth factor-BB (PDGF-BB)	GE	5′-CAGGCTACGGCACGTAGAGCATCACCATGATCCTG-3′	Amine	GO	DPV	–	0.0007–20 nM	0.65 pM	[142]
Matrix metalloproteinases (MMP-2/MMP-9)	SPE	5′-TTTTTTTCGCCGTGTAGGATTAGGCCAGGTATGGGAACCCGGTAAC-3’/5′-TTTTTTTTTTCGTATGGCACGGGGTTGGTGTTGGGTTGG-3′	Thiol	Graphene	DPV	Wound fluid	—[d]	MMP-2: 950 pg mL^{-1}/ MMP-9: 9.2 pg mL^{-1}	[143]
Thrombin	ITO	5′-GGTTGGTGTGGTTGG-3′	–	GO	PEC	Serum	100 fM - 10 nM	0.5 fM	[144]
Thrombin	SPCE	5′-AGTCCGTGGTAGGGCAGGTTGGGGTGACT-3′	–	SWCNTs	EIS	–	0.1 nM - 1 μM	0.02 nM	[145]
Thrombin	GCE	Several aptamer and/or oligonucleotide sequences applied in detection and target amplification	–	GO	SWV	Serum	100 fM - 10 nM	1.26 fM	[146]
PDGF-BB	3D carbon microelectromechanical systems microelectrode	5′-CCCCCCCAGGCTACGGCACGTAGAGCATCACCATGATCCTG-3′	Amine	rGO	CV	–	1 pM - 10 nM	0.75 pM	[147]
Alpha-fetoprotein (AFP)	SPCE	5′- GTGACGCTCCTAACGCTGACTCAGGTGCAGTTCTCGACTCGGTC TTGATGTGGGTCCTGTCCGTCCGAACCAATC-3′	Amine	Hierarchical porous Ni $(OH)_2$ NSs nanocomposite/ Hollow N-doped carbon nanoboxes ($Ni(OH)_2$@N–C n-box) nanocomposite	EIS	Serum	1 fg mL^{-1} - 100 ng mL^{-1}	0.3 fg mL^{-1}	[148]
HPV 16, biomarker of cervical cancer	GE	5′-GCAAAGGCAGCAATGTTAGCA-3′	Amine	Cu-Perylene Tetra carboxylic acid (PTCA)-rGO nanocomposite	SWV	Serum	10 fM - 10 μM	2.15 fM	[149]

[a] Real sample application not reported.
[b] Functional group of aptamer and/or oligonucleotide sequence (s) not reported.
[c] Detection technique not reported.
[d] Detection range not reported.

Table 3
Main elements used in electrochemical aptasensors equipped with gold/carbon-based nanomaterials for the detection of cancer biomarkers.

Analyte	Signal transducer	Aptamer and/or oligonucleotide sequence (s)	Aptamer functional group	Nanomaterial (s)	Detection technique (s)	Real sample	Detection range	LOD	Ref.
PSA	GCE	5′-TTTTTTTTTTATTAAAGCTCGCCATCAAATAGCTGC-3′	Thiol	rGO-Au nanocomposite	SWV	—[a]	2.5–10 ng mL^{-1}	3 pg mL^{-1}	[157]
PSA	GCE	5′- TTTTTTTTTTATTAAAGCTCGCCATCAAATAGCTGC-3′	Thiol	Carbon QDs-AuNPs nanocomposite	SWV	–	—[b]	2 fg mL^{-1}	[158]
CEA/CA 15-3	GCE	CA 15–3: 5′- GCAGTTGATCCTTTGGATACCCTGG-3’/ CEA, 1: 5′- ATACCAGCTTATTCAATT-3’/ CEA, 2: 5′- CCCATAGGGAAGTGGGGGA-3′	Amine	AuNPs-3DGH nanocomposite	DPV	Serum	CEA: 0.05–60 ng mL^{-1}/CA 15–3: 0.05–100 U mL^{-1}	CEA: 11.2 pg mL^{-1}/ CA 15–3: 11.2 × 10^{-2} U mL^{-1}	[156]
HER2	GCE	5′-AACCGCCCAAATCCCTAAGAGTCTGCACTTGTCATTT TGTATATGTATTTGGTTTTTGGCTCTCACAGACACACTACACACGCACA-3′	Amine	GQDs@AuNPs nanocomposite/ Porphyrin binuclear framework (CoP–BNF) nanocomposite	EIS	–	1–10 ng mL^{-1}	0.0489 ng mL^{-1}	[159]
HER2	GCE	5′-AACCGCCCAAATCCCTAAGAGTCTGCACTTGTCATTTTGTATATG TATTTGGTTTTTGGCTCTCACAGACACACTACACACGCACA-3′	Amine	AuNPs/Sulphur-nitrogen doped graphene quantum dots (SNGQDs)/CeO_2NPs	EIS	Serum	1–10 ng mL^{-1}	6 pg mL^{-1}	[160]
HER2/EpCAM	SPCE	EpCAM: 5′-TGAAGGTTCGTTTCGGTGGGTGTAGACTCTTTAGAAGA GATACAGATTTTGGGAATGTTTTTGCTAGAAGGAAACAGTTAC-3’/HE R2: 5′-CCGCAACCACGACCGAAAGACAACGCAATCTGACACGTGGTT TTTTTTGCTATTCAACGCTGAGACATGACG-3′	Thiol	MWCNTs/AuNPs	DPV	Cell exosomes	10–2 × 10^{10} particle mL^{-1}	1 particle mL^{-1}	[57]
CA 15-3	GCE	5′-CCAGGGTATCCAAAGGATCAACTGC-3’/5′- GCAGTTGATCCTTT GGATACCCTGG-3’/5′- GCAGTTGATCCTTTGGATACCCTGG-3′	Thiol	AuNPs-Magnetic graphene nanocomposite	SWV	Serum	100 fM - 100 nM	9.4 fM	[161]
CA 15-3	GCE	5′- GCAGTTGATCCTTTGGATACCCTGGTTTT-3′	Thiol	Au@rGO nanocomposite	DPV	MCF-7 breast cancer cell line	0.5–5000 pg mL^{-1}	0.085 pg mL^{-1}	[162]
CA 15-3	GCE	—[c]	Thiol	MnO@C@AuNPs nanocomposite/AgNPs	DPV/CA	Serum	DPV: 0.001–100 nM/CA: 0.001–10 nM	DPV: 0.31 pM/CA: 0.25 pM	[80]
Tumorous exosomes related to breast cancer MCF-7 cells	GCE	5′-TTTTTTTTTTTTTTTTTTTTTTTTTTTTTTTCTCTTCTCCGAGCC GGTCGAAATAGTCACCCCACCTCGCTCCCGTGACACTAATGCTA TTTTTTTTTTTTTTTTTTTTTTTTTTTTTTTCTCTTCTCCGAGCCGGTCGAAATAGT-3′	—[d]	Porous carbon nanostructure/Au NPs	DPV	Serum	5 × 10^4–1 × 10^8 particles mL^{-1}	1.6 × 10^4 particles mL^{-1}	[155]
17β-Estradiol	Paper-based electrode	5′- GCTTCCAGCTTATTGAATTACACGCAGAGGGTAGCGGCT CTGCGCATTCAATTGCTGCGCGCTGAAGCGCGGAAGC-3′	Biotin	rGO-thionine-SA-AuNPs-CS nanocomposite	DPV	Serum	10 pg mL^{-1} - 100 ng mL^{-1}	10 pg mL^{-1}	[163]
Glypican-3	SPE	5′- TAACGCTGACGCTGACCTTAGCTGCATTTTACATGTTCCA-3′	Amine	rGO-Hemin nanocomposite/AuNPs	DPV	Serum	1–10,000 ng mL^{-1}	2.86 ng mL^{-1}	[164]
Glypican-3	Si-based chip	5′-TAACGCTGACCTTAGCTGCATGGCTTTACATGTTCCA -3’/5′-ACCATGGTTCGGTTTGGCGTACTACTACTTACTAACC-3′	–	rGO-PEI-AuNPs nanohybrid nanocomposite	Potentiometry	Serum	0.1–100 μg mL^{-1}	40 ng mL^{-1}	[165]
Leukemia	SPE	5′-ATCTAACTGCTGCGCCGCCGGGAAAATACTGTACGGTTAGA-3′	Thiol	Copper sulfide-(CuS) graphene nanocomposite/Au-graphene nanocomposite	DPV	CCRF-ECM cells in blood samples	50–1 × 10^6 cell mL^{-1}	18 cell mL^{-1}	[151]

(*continued on next page*)

Table 3 (*continued*)

Analyte	Signal transducer	Aptamer and/or oligonucleotide sequence (s)	Aptamer functional group	Nanomaterial (s)	Detection technique (s)	Real sample	Detection range	LOD	Ref.
Programmed death-ligand 1	Paper-based microfluidic device	5′- GCTGTGTGACTCCTGCAAGACGGACCAGCCTTGCCGCAAGACGGAC CAGGGATTCAAACGAGCAGCTGTATCTTGTCTCC-3′	Thiol	NH_2-SWCNT nanocomposite/AuNPs	DPV	Serum	10 pg mL^{-1} - 2.5 ng mL^{-1}	10 pg mL^{-1}	[166]
MCF-7 breast cancer cells	GCE	5′-TTTGGTGGTGGTGGTTGTGGTGGTGGTGG-3′	Amine	GO–CS–AuNPs nanocomposite	EIS	–	1×10^1–1×10^6 cells mL^{-1}	4 cells mL^{-1}	[167]
Golgi protein 73	SPCE	5′-CCCCCGCAGTTGATCGTTTGGATACCCTGG-3′ /5′-ACGGTCGGA TGCCACTACAGTTGGTTTTTTTTTTGTTATTTAGAG TAAAAACCTTGTGTGTAGTGACTCATGGACGTGCTGGTGAC-3′	Amine	H-rGO-Mn_3O_4 nanozyme nanocomposite/ Gold@poly (o-phenylenediamine) nanohybrid nanocomposite	SWV	Serum	0.01–100 ng mL^{-1}	0.0071 ng mL^{-1}	[168]
C-reactive protein	GCE	5′- CGAAGGGGATTCGAGGGGTGATTGCGTGCTCCATTTGGTG-3′	Thiol	AuNPs@C-Zeolite imidazole framework (ZIF)-67 nanocomposite	DPV	Plasma	10 pg mL^{-1} - 10 μg mL^{-1}	0.44 pg mL^{-1}	[169]

[a] Real sample application not reported.
[b] Detection range not reported.
[c] Aptamer and/or oligonucleotide sequence (s) not reported.
[d] Functional group of aptamer and/or oligonucleotide sequence (s) not reported.

4.3. Multiplexed electrochemical aptasensor (s) equipped with gold/carbon-based nanomaterials

In a research, an aptasensor was developed on a SPCE to diagnose breast cancer using the detection of exosome biomarkers [57]. First, a nanocomposite was synthesized from a mixture solution containing dissolved CS in acid, amine-functionalized multi-walled carbon nanotubes (MWCNTs), and ionic liquid, which modified the surface of the signal transducer. Then, a thin layer of AuNPs was electrodeposited (via a CA procedure) on the surface of SPCE/MWCNT-IL-CS. Afterward, a thiol functionalized aptamer was immobilized on the surface of the electrode and established Au–S covalent bond with AuNPs, and at this point, the main part of the aptasensor was developed (SPCE/MWCNT-IL-CS/AuNPs/aptamer). In the next step, various breast cancer exosomes were added to the surface and captured partially by aptamer strands. At the next step, two other aptamers related to EpCAM and HER2 were added to the surface. Then, these sequences contributed to a RCA signal amplification cycle directed by a particular circular DNA template. Applying RCA led to enriching the contributed sequences with guanine and thymine. The final EpCAM aptamer interacted with the lead ion, and the final HER2 aptamer interacted with the copper ion. Here, the DPV technique was applied to measure various concentrations of the analytes. Enhancing various concentrations of analytes reflected more ions in the detection medium, which was a reason for increasing DPV peak currents (signal-on). This multiplexed aptasensing system could detect EpCAM and HER2 exosome biomarkers in a linear range from 10 to 2×10^{10} particles mL^{-1} and with a LOD equal to 1 particles mL^{-1}.

Another multiplexed aptasensor has been designed to simultaneously detect CA 15–3 and CEA [156]. First, a GCE modified with AuNPs-3D graphene hydrogel (AuNPs-3DGH) nanocomposite was applied as the signal transducer. Afterward, a mixture of two aptamers related to analytes was added to the surface. In the next step, the analytes were added. Finally, two bioconjugated structures containing structure 1 (CA-aptamer-AuNPs-Fc-graphene) and structure 2 (CEA-Apt2-AuNPs-hemin-graphene hybrid NSs) were added to the surface, and the analytes were located in a sandwich-like position. Since the redox agents contributed in structure-1 and structure-2 were not the same, different DPVs were produced for each analyte in a signal-on pattern.

Table 3 presents the critical features of electrochemical aptasensors designed to detect cancer biomarkers equipped with gold/carbon-based nanomaterials. Classifications were mainly based on the type of cancer analyte, signal transducer, and other vital features.

5. Electrochemical aptasensors equipped with other nanomaterials for the detection of cancer biomarkers

5.1. CEA electrochemical aptasensor (s) equipped with other nanomaterials

In another aptasensor for CEA detection, a thiol-functionalized capture probe (c-DNA) was immobilized on the surface of a GE [170]. Then, an aptamer was added and could be hybridized with the c-DNA. At the next step, the CEA was added, and due to the high affinity between aptamer and analyte, the hybridized structure was cleaved. The released aptamer strands captured the analyte molecules. On the other side, via contributing several single-stranded DNA sequences, a dendrimer-like DNA nanoassembly was produced and added to the surface of the signal transducer to interact and hybridize with c-DNA molecules. Finally, the electrochemical assays were followed by DPV and in the presence of hydroquinones, hemin, and H_2O_2 agents. The presence of more analyte molecules processed the increase of free c-DNA strands for hybridization with the dendrimer-like DNA nanoassembly; this nanoassembly carried more redox agents, and consequently, DPVs signals were enhanced (signal on).

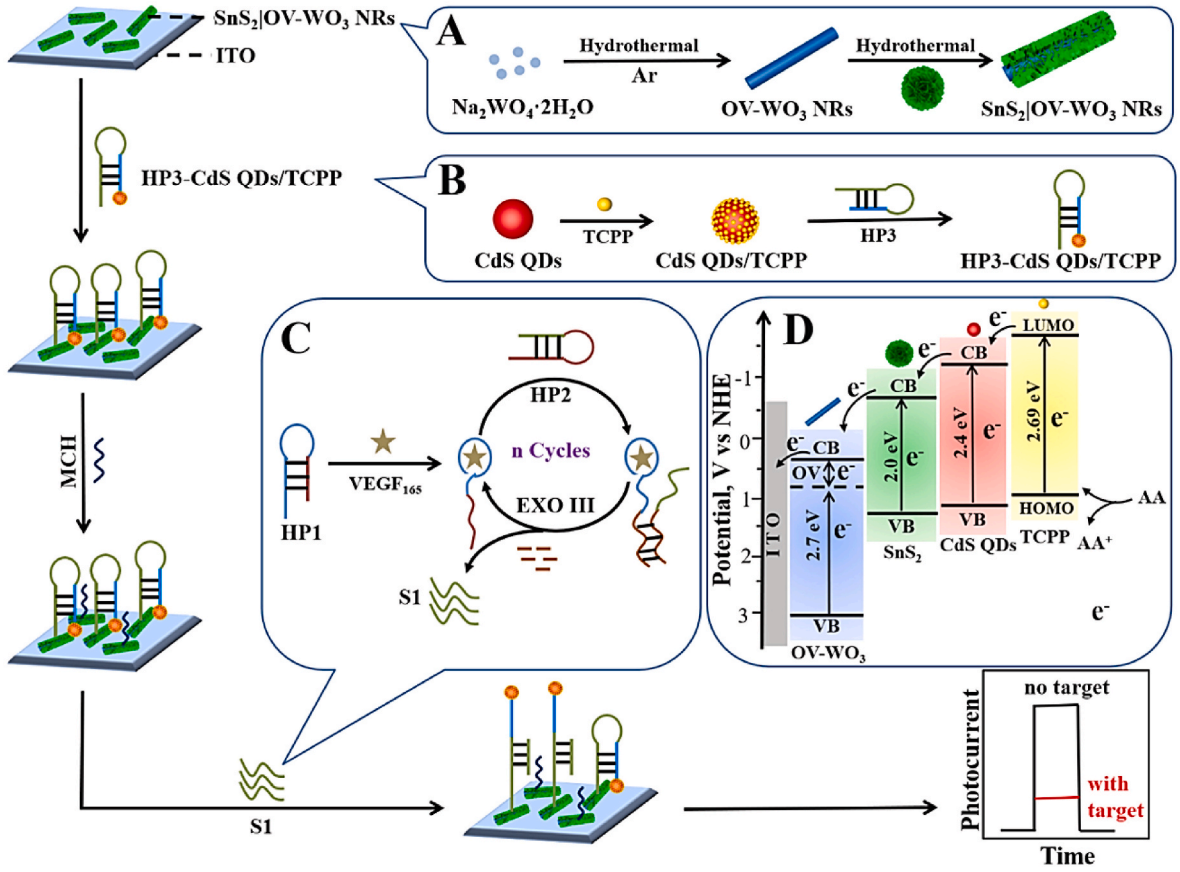

Fig. 4. Schematic illustration of a VEGF electrochemical aptasensor developed on the surface of an ITO electrode; preparation of SnS_2-OV-WO_3 nanocomposite and modifying the surface **(A)**; conjugation of a hairpin aptamer with CdS QDs **(B)**; performing target recycling method **(C)**; electron transfer pathways from the surface of the signal transducer **(D)**; License Number: 5430261456120.

5.2. VEGF electrochemical aptasensor (s) equipped with other nanomaterials

VEGF is a cancer biomarker that is often used to diagnose and monitor certain types of cancers such as lung, breast, gastric, ovary, colon, and rectum. This biomarker is produced by cancer cells and plays a critical role in the formation of new blood vessels that supply nutrients and oxygen to tumors [171,172]. The levels of VEGF in the blood or tumor tissue can be measured to help diagnose cancer and monitor its progression. There is no specific "normal range" for VEGF levels as it can vary depending on several factors such as age, gender, health status, and underlying medical conditions. Elevated levels of VEGF in the blood or tumor tissue may indicate the presence of cancer or the potential for tumor growth and metastasis. Overall, VEGF is an important biomarker in cancer diagnosis, prognosis, and treatment [173,174].

In a research, the detection of VEGF was followed by a dual signal amplification-based aptasensor [175]. Here a GE was used as the signal transducer and was treated with a thiol-functionalized DNA sequence (anchor DNA). In the next step, another DNA sequence (capture probe) was mixed with the analyte and added to the surface of the working electrode. Then, the report-probe was added. The report-probe contained two carboxyl-functionalized DNA sequences (HP1 and HP2) and CeO_2 NPs. As the last step, the replacement DNA (r-DNA) sequence was added, and the HCR was activated. The electrochemical assays were followed by DPV. The presence of CeO_2 NPs catalyzed H_2O_2 to produce the sensing signal (signal-on).

In another research, a PEC-based aptasensor has been developed to detect VEGF [176]. In this research, an ITO electrode modified with hierarchical tin sulfide-oxygen vacancy-tungsten trioxide (SnS_2-OV-WO_3) NRs nanocomposite was used as the signal transducer (Fig. 4). In the proposed platform, a conjugated structure was synthesized from a mixture of a thiol/carboxyl functionalized hairpin aptamer (HP3) and CdS QDs. Then the prepared mixture was immobilized on the electrode surface. On the other side, the analyte and two other oligonucleotide sequences (HP1 and HP2) were associated with an enzyme-assisted target amplification cycle; the output DNA (S1) was added to the surface and was led to open the hairpin structure of HP3. The opened form of HP3 led to a change in the position of CdS QDs at a far distance from the surface of the signal transducer, and this event reduced the output PEC signal intensity (signal off).

5.3. Tumor exosomes electrochemical aptasensor (s) equipped with other nanomaterials

In a research, the detection of tumorous exosomes related to breast cancer MCF-7 cells was followed by an aptasensing platform [177]. A GE was used as the signal transducer and treated with a thiol-functionalized aptamer. Then, the analyte was added to the surface. In another way, two H shape-like DNA units were hybridized, activating a multidirectional HCR signal amplification and creating a DNA nanostructure. Afterward, the DNA nanostructure was added to the surface of the signal transducer, which could absorb a large amount of SA-horseradish peroxidase (SA-HRP) in the analysis medium (through the reaction between SA and biotin). At the same time, the HRP catalyzed the required redox reaction to detect the analyte. The electrochemical assays were followed by the CA (signal-off).

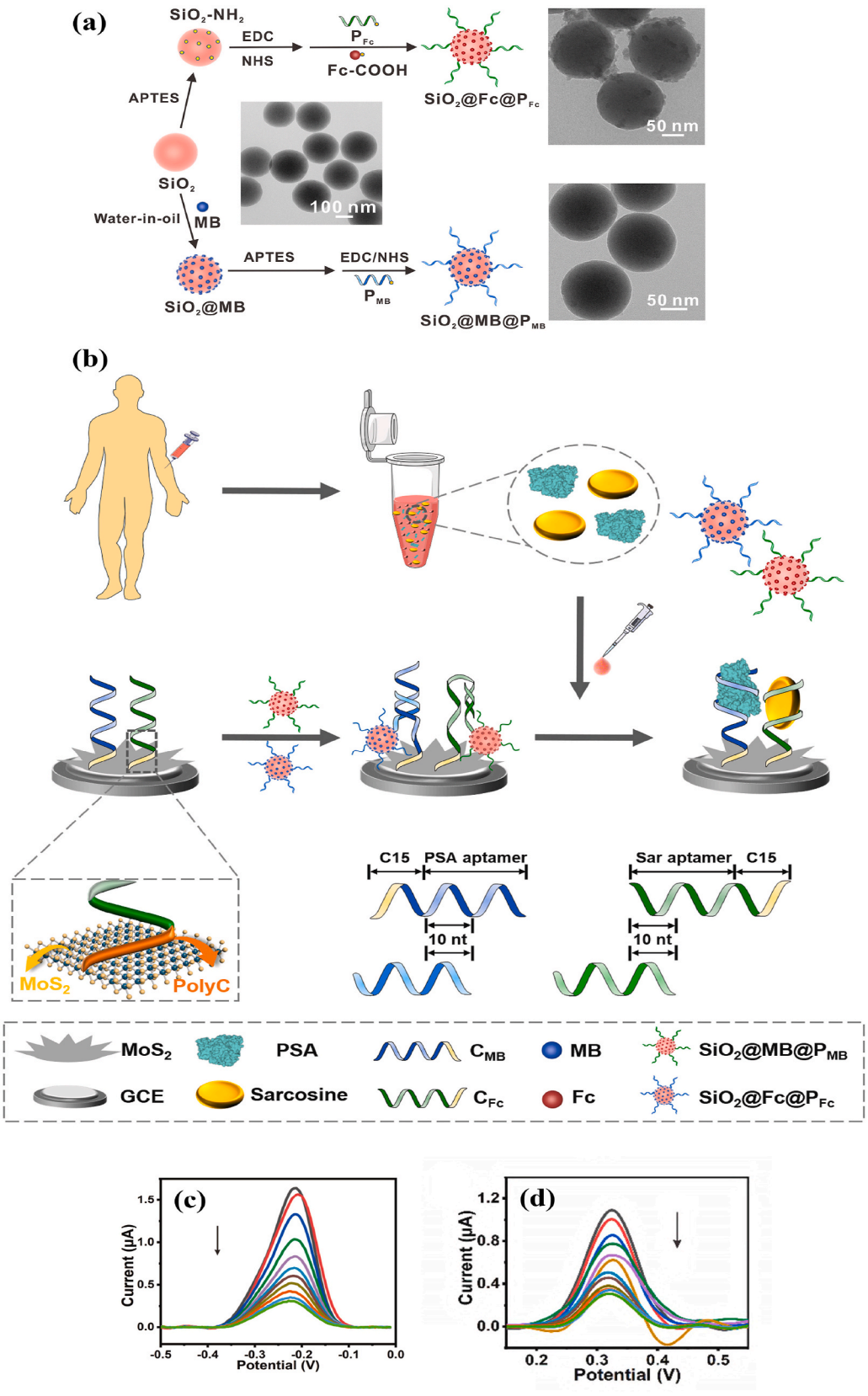

Fig. 5. Schematic presentation of an electrochemical aptasensor for detection of PSA and sarcosine; preparation of two core-shell nanocomposites (SiO_2@MB@P_{MB} and SiO_2@Fc@P_{Fc}) as signal amplifier nanoprobes **(a)**, designing the aptasensing platform including modification of a GCE with MoS_2 nanoflowers, immobilization of capture probes, hybridization with signal amplifier nanoprobes, and binding with the analyte molecules **(b)**, SWV measurement of PSA **(c)**, and SWV measurement of Sarcosine **(d)**; License Number: 5430250166451.

Table 4
Main elements used in electrochemical aptasensors equipped with other nanomaterials for the detection of cancer biomarkers.

Analyte	Signal transducer	Aptamer and/or oligonucleotide sequence (s)	Aptamer functional group	Nanomaterial (s)	Detection technique (s)	Real sample	Detection range	LOD	Ref.
PSA/Sarcosine	GCE	Several aptamer and/or oligonucleotide sequences applied in detection and target amplification	Carboxyl	MoS_2 nanoflowers/ SiO_2nanoprobes	SWV	Serum	PSA:1 fg mL^{-1} - 500 ng mL^{-1}/ Sarcosine: 1 fg mL^{-1} - 1 μg mL^{-1}	PSA: 1.21 fg mL^{-1}/ Sarcosine: 3.4 fg mL^{-1}	[178]
CEA	GE	5′-CCACGATACCAGCTTATTCAATTCGTGG-3′	Carboxyl	Zirconium-cobalt MOF nanocomposite	EIS/DPV	Serum	0.001–100 pg mL^{-1}	0.35 fg mL^{-1}	[180]
CEA	GE	Several aptamer and/or oligonucleotide sequences applied in detection and target amplification	Thiol	3D DNA nanoprobe	DPV	Serum	10 fg mL^{-1} - 50 ng mL^{-1}	4.88 fg mL^{-1}	[181]
CEA	GE	Several aptamer and/or oligonucleotide sequences applied in detection and target amplification	Thiol	DNA nanostructure	DPV	Serum	1–30,000 pg mL^{-1}	0.045 pg mL^{-1}	[182]
CEA	GE	Several aptamer and/or oligonucleotide sequences applied in detection and target amplification	Thiol	DNA nanostructure	DPV	Serum	2–45 ng mL^{-1}	0.24 ng mL^{-1}	[170]
CEA	Magnetic gold-disk electrode	5′-ATACCAGCTTATTCAATT-3′	Amine	Magnetic beads	EIS/pH meter assay	Serum	0.01–100 ng mL^{-1}	9.3 pg mL^{-1}	[183]
CEA	GCE	5′-ATACCAGCTTATTCAATT-3’/5′- TTTTTTAATTGAATAAGCTGGTAT-3′	Thiol	AgNCs	ECL	Serum	100 ag mL^{-1} - 10 ng mL^{-1}	38.86 ag mL^{-1}	[184]
CEA	Fluorine-doped tin dioxide (FTO)	5′-AACATCTTCTACACATGGAGATGTTGATTGAACCATGTGTAGA-3’/5′ -CATACCAGCTTATTCAATTCA-3′	Amine/ Biotin	BiOI-α-Fe_2O_3 NSs array nanocomposite	PEC	Serum	1×10^{-4} - 20 ng mL^{-1}	36.89 fg mL^{-1}	[185]
HER2	GCE	5′-CCCCCCAACCGCCCAAATCCCTAAGAGTCTGCACTTGTCATTTTGTATAT GTATTTGGTTTTTGGCTCTCACAGACACACTACACACGCACA-3′	Amine	CeO_2 NPs	EIS	Serum	1–10 ng mL^{-1}	0.2 ng mL^{-1}	[186]
HER2	GCE	5′-GCAGCGGTGTGGGG-3′	—[a]	Antimonite nano flakes/Zeolitic imidazolate frameworks nanocomposite	DPV	Serum	0.5–1000 pg mL^{-1}	155 fg mL^{-1}	[187]
HER2	GE	5′-AACCGCCCAAATCCCTAAGAGTCTGCACTTGTCATTTTGTATATGT ATTTGGTTTTTGGCTCTCACAGACACACTACACACGCACA-3′	–	MXene NSs/$CoFe_2O_4$@Ag magnetic nanohybrids nanocomposite	DPV	SK-BR-3 cells	10^2 -10^6 cells mL^{-1}	47 cells mL^{-1}	[188]
HER2/ Estrogen receptor (ER)	ITO	HER2: 5′-GCAGCGGTGTGGGG-3’/ER: 5′-GTCAGGTCACAGTGACCTGA TCAAAGTTAATG-3′	–	Antimony (Sb) quantum dots@ZIF-67 nanocomposite	SWV	Serum	0–10 pg mL^{-1}	HER2: 3.4 fg mL^{-1}/ HER2/ER: 6.9 fg mL^{-1}	[189]
HER2/EpCAM	MGCE	HER2: 5′-GCAGCGGTGTGGGG-3’; 5′- CCCCACACCGCTGC-3’/EpCAM: 5′-CACTACAGAGGTTGCGTCTGTCCCACGTTGTCATGGGGGGTTGGCCTG-3’; 5′-GACGCAACCTCTGTAGTG-3′	Thiol	Ag–Ru nanocomposite/Ag–Pt nanocomposite	DPV	Serum	HER2: 1–500 pg mL^{-1}/ EpCAM: 1 pg mL^{-1} - 100 pg mL^{-1}	HER2: 0.6 pg mL^{-1}/ EpCAM: 0.3 pg mL^{-1}	[179]
CA 15-3	GCE	5′- TTTTTGCAGTTGATCCTTTGGATACCCTGG-3’/5′- TTTCACCCCAC CTCGCTCCCGTGACACTAATGCTA-3′	Amine	Ru $(bpy)_3^{2+}$@SiO_2 NPs nanocomposite	ECL	Serum	3.22×10^{-4} - 156 μg mL^{-1}	2.73×10^{-4} μg mL^{-1}	[190]
Tumorous exosomes related to breast cancer MCF-7 cells	SPE	5′-CACCCCACCTCGCTCCCGTGACACTAATGCTAAGTAGTGGGGTG-3’/5′-TTAGGGTTAGGGTTAGGGGTGTAGGCTATCAACACCCCACTACTTTAGGG-3’/5′-TTAGGGTTGATAGCCTACACAGTAGTGGGGTGTAGGGTTAGGGTTAGGG-3′	–	Zr-MOFs nanocomposite	DPV	Exosomes	1.7×10^4–3.4×10^8 particles mL^{-}	5×10^3 particles mL^{-1}	[191]
Tumorous exosomes related to breast	GE	5′-TGAAGGTTCGTTGTTTCGGTGGGTGTAGACTCTTTAGAAG AGATACAGATTTTGGGAATG-3′	Thiol	DNA nanostructure	CA	Serum	5×10^2–1×10^5 exosomes μL^{-1}	285 exosomes μL^{-1}	[177]

(*continued on next page*)

Table 4 (*continued*)

Analyte	Signal transducer	Aptamer and/or oligonucleotide sequence (s)	Aptamer functional group	Nanomaterial (s)	Detection technique (s)	Real sample	Detection range	LOD	Ref.
cancer MCF-7 cells									
Tumorous exosomes	ITO	Several aptamer and/or oligonucleotide sequences applied in detection and target amplification	Thiol/ Biotin	CuO NPs/Magnetic beads	PEC	Serum	5×10^3–1×10^6 particles μL^{-1}	1.38×10^3 particles μL^{-1}	[192]
VEGF	GE	5′-CCCTGCACTCTTGTCTGGAAGACGG-3’/5′-ACTCTTGTCTGGA AGACGGAAACCCTGCACTCCCGTCTTCCAGACAAGAGTGCAGGG-3′	Thiol	CeO_2 NPs	DPV	Tear	10 fg mL^{-1} - 0.1 ng mL^{-1}	7.39 fg mL^{-1}	[175]
VEGF	GE	5′-TTTCCCGTCTTCCAGACAAGAGTGCAGGG-3′	–	Melem- hexaketocyclohexane octahydrate (represented as M–HO–COF) nanocomposite	EIS	Serum	1 fg mL^{-1} - 10 ng mL^{-1}	49 cells mL^{-1}	[193]
VEGF	GCE	5′-AAAAAAAAAACCGTCTTCCAGACAAGAGTGCAGGGAAAAAGAAGACGG-3′	Carboxyl	Pt–Pd–MoO_2 nanocomposite	EIS	Fetal bovine serum	10 pg mL^{-1}- 1 μg mL^{-1}	8.2 pg mL^{-1}	[194]
VEGF	ITO	5′-CCACACCAACCTCTTCGTTTCTTCCTGGGGGAGTATTGCGGAGGAAGG-3’/5′-CAACCTCTTCGTAGAGAGGTGTTTCCGAAGAGGTTGGTGTGG-3’/5′-GCAGTCTAGAAACACCTCTCTACGAAGAGGTTGTAGACTGC-3′	Thiol/ Carboxyl	SnS_2-OV-WO_3 NRs nanocomposite/CdS-QDs nanocomposite	PEC	Serum	0.5 fM - 10 nM	0.34 fM	[176]
TNF-α	ITO	5′-TGGTGGATGGCGCAGTCGGCGACAA-3′	Amine	Molybdenum disulfide QDs-zeolitic imidazolate framework-8@ZnO nanorod arrays (MQDs-ZIF-8@ZnO NR) nanocomposite	PEC/DPV	Serum	PEC: 5 fg mL^{-1}- 5 μg mL^{-1}/DPV: 10 fg mL^{-1} - 0.5 μg mL^{-1}	PEC: 1.46 fg mL^{-1}/ DPV: 6.14 fg mL^{-1}	[195]
CA-125	MGCE	5′-TTTTTTTTTTTTTTTTTTTTCCCTATAGTGAG-3′	Thiol	Magnetic α-Fe_2O_3–Fe_3O_4heterogeneous hollow NRs nanocomposite	DPV	Serum	5–125 U mL^{-1}	2.99 U mL^{-1}	[196]
AFP	Au-n-type gallium nitride photoelectrode	5′- GTGACGCTCCTAACGCTGACTCAGGTGCAGTTCTCGACTCGGTCTT GATGTGGGTCCTGTCCGTCCGAACCAATC-3′	Thiol	MoS_2NSs	PEC	Serum	1–150 ng mL^{-1}	0.3 ng mL^{-1}	[197]
CD20 cells (marker related to lymphoma)	GE	5′-GGAGGATAGTTCGGTGGCTGTTCAGGGTCTCCTCCT-3′	Thiol	Luminol-(L)–CS–Pt NPs nanocomposite	ECL	Whole blood	70 - 2090 cells mL^{-1}	31 cells mL^{-1}	[198]
Folate receptor-HeLa cells	GE	—[b]	Thiol	Pt@BSA nanocomposite	DPV	—[c]	2.8×10^1–2.8×10^6 cells mL^{-1}	9 cells mL^{-1}	[199]
Cytokeratin fragment antigen 21–1	GE	Several aptamer and/or oligonucleotide sequences applied in detection and target amplification	Thiol/ Amine	Magnetic beads	DPV	Serum	10 pM - 1 μM	8.079 pM	[200]
Progastrin-releasing peptide	GCE	5′-CATGCGGAGTAGATTCGAGCCCAGATAGTCCCTGGTTATTTCCTTAGG-3′	Thiol	AgNPs/Antimony@TiO_2 nanocomposite	ECL/DPV	Serum	10 fg mL^{-1} - 12 ng mL^{-1}	1.3 fg mL^{-1}	[201]
ApoA1	SPCE	5′-CTATAGCAATGGTACGGTACTTCCCCTCGGCACGTTCTCAGTAGCGC TCGCTGGTCATCCCACACAAAAGTGCACGCTACTTTGCTAA-3′	Amine	MoS_2–ZrO_2 nanocomposite	ECL	Serum	0.1–1000 pg mL^{-1}	53 fg mL^{-1}	[202]
HER2	SPCE	5′-GGGCCGTCGAACACGAGCATGGTGCGTGGACCTAGGATGACCTGAGTACTGTCC-3′	–	Antimonene@ZIF-67 nano composite	SWV	Serum	0–1000 pg mL^{-1}	4.853 fg mL^{-1}	[203]
AFP	GE	5′-GGCAGGAAGACAAACAGCTTGGCGGCGGGAAGGTGTTTAAATTCCCGGG TCTGCGTGGTCTGTGGTGCTGT-3’/5′-ATGCCGATCCCCAAAAGTGTACACT TAATCGAAGCTTT-3’/5′-AAAGCTTCGATTAAGTGTACACTTTTGGGGATCGGCAT-3′	Thiol/ Amine	CdS QDs/Lens culinaris agglutinin@AgNPs nanocomposite	DPV	Serum	0.0004–40 ng mL^{-1}	0.51 pg mL^{-1}	[204]

(*continued on next page*)

Table 4 (*continued*)

Analyte	Signal transducer	Aptamer and/or oligonucleotide sequence (s)	Aptamer functional group	Nanomaterial (s)	Detection technique (s)	Real sample	Detection range	LOD	Ref.
HER2	GCE	5′-GCAGCGGTGTGGGG-3′	–	ZIF-67@PDA nanocomposite	DPV	Serum	0.75–40 pg mL^{-1}	44.8 fg mL^{-1}	[205]
HER2/ER	ITO	HER2: 5′-GCAGCGGTGTGGGG-3′/ER: 5′-GTCAGGTCACAGTGACCTGATCAAAGTTAATG-3′	–	Co-MOF NSs	SWV	Serum	0–15 pg mL^{-1}	HER2: 3.8 fg mL^{-1}/ER: 6.8 fg mL^{-1}	[206]
Melanoma B16–F10 cells	GE	5′-ATCTAACTGCTGCGCGCCGGGAAAATACTGATCGGTTAGA-3′	–	CoCu-ZIF@carbon dots nanocomposite	EIS	–	1×10^2–1×10^5 cells mL^{-1}	33 cells mL^{-1}	[207]
Protein tyrosine kinase-7	SPGE	5′-ATCTTACTGCTGCGCGCGGGAAAATACTGTACGGTTAGATTTTTTTTTT-3′	Amine	AuNPs	DPV	Serum	100 fM - 10 pM	100 fM	[208]

[a] Functional group of aptamer not reported.
[b] Aptamer and/or oligonucleotide sequence (s) not reported.
[c] Real sample application not reported.

5.4. Multiplexed electrochemical aptasensor (s) equipped with other nanomaterials

In a research, an aptasensing platform was designed to detect PSA and sarcosine as two important prostate cancer biomarkers [178]. In order to set up aptasensing elements, as the first step, MoS_2 nanoflowers were synthesized from MoO_3 powder via a hydrothermal method. This nanostructure was used for modification of the signal transducer surface. In another procedure, SiO_2 NPs were synthesized and employed to produce two core-shell nanocomposites as signal amplifier nanoprobes ((MB-doped SiO_2 NPs conjugated with a carboxyl-functionalized aptamer (P_{MB}) sequence (SiO_2@MB@P_{MB})) and (SiO_2@Fc conjugated with a carboxyl-functionalized aptamer (P_{Fc}) sequence (SiO_2@Fc@P_{Fc})) (Fig. 5). Here, a GCE was used as the working electrode and modified with MoS_2 nanoflowers through the drop-casting procedure. Then, two aptamer sequences (capture probes) were immobilized on the electrode surface. Subsequently, the produced core-shell nanoprobes were added, and P_{MB} and P_{Fc} could be interacted with and hybridized with capture probes (Fig. 5). Finally, various concentrations of analytes were added, and electrochemical assays were monitored via the SWV technique. In the absence of analytes, the core-shell nanoprobes could be hybridized with the aptamer strands on the electrode surface and could produce strong electrochemical signals related to MB and Fc as redox agents. In comparison, in the presence of analytes, due to the higher affinity between capture probes and analytes, most core-shell nanoprobes released from the surface of the electrode and replaced with analyte molecules which this event was led to reducing the conductivity of the surface and decreasing SWV peak currents (signal-off). The presented aptasensor detected PSA and sarcosine in a linear range from 1 fg mL^{-1} to 1 ng mL^{-1} (LOD: 2.5 fg mL^{-1}) and 1 fg mL^{-1} to 1 ng mL^{-1} (LOD: 14.4 fg mL^{-1}), respectively.

A multiplexed aptasensor was designed to simultaneously detect HER2 and EpCAM [179]. First, AgRu NPs and AgPt NPs were synthesized. AgRu NPs were applied in a conjugated structure in the presence of a thiol-functionalized aptamer (HER2-Apt-A). On the other side, AgPt NPs were used in the presence of another thiol-functionalized aptamer (EpCAM-Apt-A). In another procedure, complementary strands (HER2-Apt-C and EpCAM-Apt-C) were prepared in a conjugated form with Au–Fe_3O_4–Ni-MOF NSs nanocomposite. At the next step, a mixture of all prepared conjugated structures was immobilized on the surface of a MGCE as the signal transducer. Then, various concentrations of analytes were added, and electrochemical measurements were followed by DPV. In the absence of analytes, aptamers A were hybridized with aptamers C. In the presence of analytes, due to higher affinity, aptamers A released from the surface and captured the analyte molecules. This event reduced the electron transfer facilitated by AgRu NPs and AgPt NPs (signal off for both analytes).

Table 4 presents the critical features of electrochemical aptasensors designed to detect cancer biomarkers equipped with other nanomaterials. Classifications were mainly based on the type of cancer analyte, signal transducer, and other vital features.

6. Analysis of main features/elements of cancer aptasensing platforms

In a deep analysis, essential features related to all included research were evaluated. The outputs of this comprehensive assay can be very applicable as a shortcut to designing subsequent electrochemical aptasensing platforms. As evident in the review, we included only research published in 2021–2023. The first analysis confirmed that about 44% of all research in this field aimed to detect four important cancer biomarkers, including CEA, HER2, CA 15–3, and PSA (Fig. 6, a). This result shows the interest and importance of these biomarkers for the diagnosis and prognosis of cancers. In another analysis, the type of employed signal transducers in electrochemical measurements was investigated. The results confirmed that the most reliable electrodes used in recent

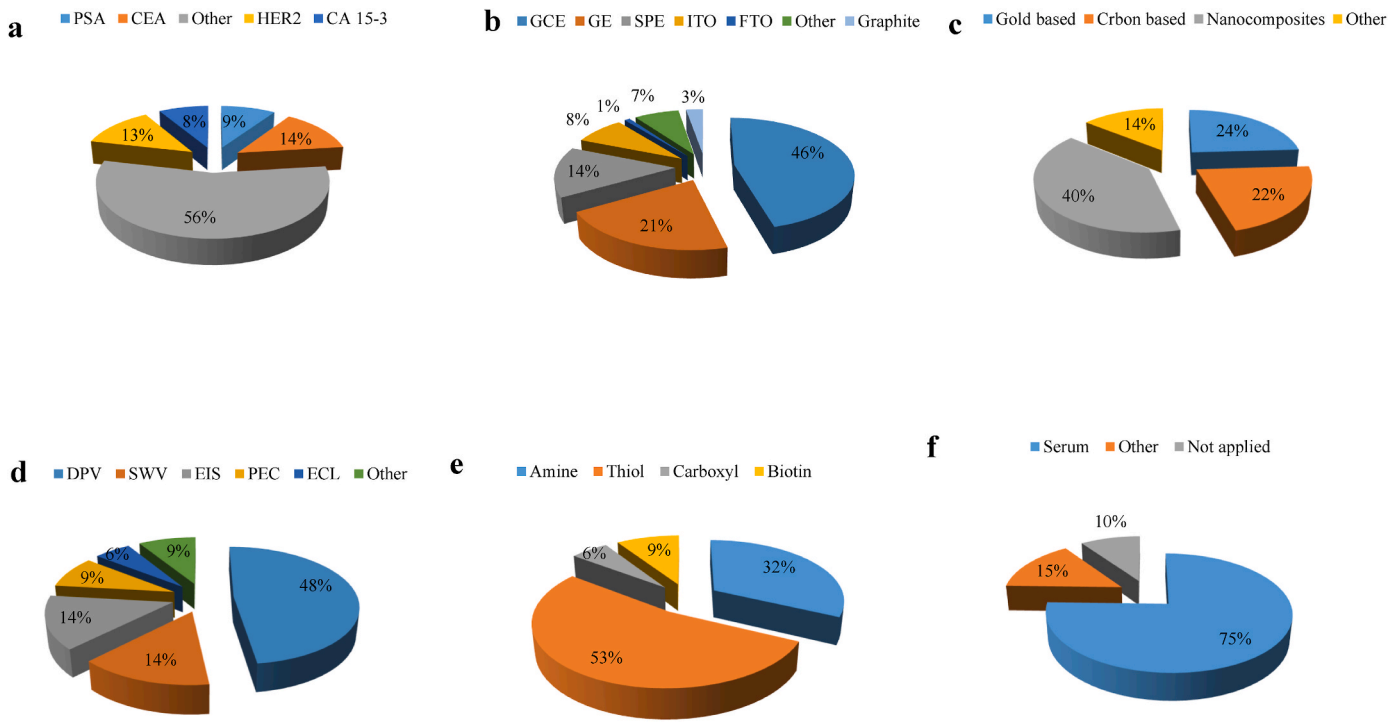

Fig. 6. Analysis of prominent features in recent electrochemical aptasensors developed for detection of cancer biomarkers; cancer biomarkers **(a)**; signal transducers **(b)**; nanomaterials **(c)**; detection technique **(d)**; the functional group of aptamers **(e)**; and real sample application **(f)**.

research included GCE (46%), GE (21%), and various types of SPE (14%), which shows that at least about 81% of all used signal transducers were commercial (Fig. 6, b). The results of another analysis reflect that most researchers found innovations in substances, such as using advanced materials, new platforms of the biorecognition element, or promising assemblies in aptasensing platforms. In another analysis, various types of used nanomaterials were categorized, and it was found that various nanocomposites (40%), gold-based nanomaterials (24%), and carbon-based nanomaterials (22%) were the most employed nanomaterials (Fig. 6, c). This analysis shows that the aim for using nanocomposites was the convergence of synergic effects of several nanomaterials simultaneously. This application keeps these advanced materials' functional role in the desired state to improve the sensing sensitivity and final detection performance. The main reasons for using gold and carbon-based nanomaterials are biocompatibility, ease to use, high stability, and high conductivity. In another analysis, the type of used electrochemical detection techniques was categorized, and the results confirmed that most of the research was concluded through DPV (48%), EIS (14%), and SWV (14%) techniques which can be highlighted as a guide for the subsequent research (Fig. 6, d). The functionalization of aptamer and/or oligonucleotide sequence (s) with special chemical groups is used as a linker to connect them to anticipated substrates, such as the surface of the signal transducer or desired parts of the biorecognition element. In included research, the most applied functional group integrated to aptamer and/or oligonucleotide sequence (s) were thiol (53%), amine (32%), biotin (9%), and carboxyl (6%), which this analysis showed a direct association with the type of employed surfaces also (Fig. 6, e). In the last analysis, the most used type of real samples was categorized. In 75% of all recent electrochemical aptasensing platforms, serum samples were considered as the real sample application (Fig. 6, f). This significant result confirms that accurate monitoring of most cancers was possible via analyzing serum samples.

7. Conclusion and future perspectives

Today, cancer is one of the biggest challenges for human society. Unfortunately, there are huge costs involved in controlling this disease per year. Prevention of exposure to cancer risk factors, early diagnosis of cancers, and adopting the appropriate treatment paths are ways to deal with this deadly disease. Biomarkers concentrations in biofluids can be explicitly used to diagnose various cancers. Therefore, molecular detection of these biomarkers is one of the best and newest methods for the early detection of cancers. In aptasensors, aptamers as the biorecognition element are designed with high specificity against cancer biomarkers. Several optimizations have been recently used to design these aptasensors, including the application of nanomaterials due to their unique physicochemical properties and biomolecular amplification and editing techniques against probe sequences or nucleotide analytes. Some recent research has also monitored the simultaneous diagnosis of several cancer biomarkers (multiplexed aptasensors). There are different designs in the platforms of these biosensors, all of which aim to provide the optimal diagnosis of cancers.

Aptasensors currently face several critical challenges. One of these challenges is the temporal and environmental sustainability of the biological components involved in their structure. In addition, the stability of aptamers in the used solutions and electrolytes must also be considered. Another challenge is to predict the reproducibility and selectivity to be verified in different media, especially to detect real samples. Trust in clinical diagnostic systems is not easy to achieve, and these challenges must be addressed before commercializing these products. In subsequent research, more focus should be placed on improving the performance of aptasensors for detecting analytes in real samples.

As aptasensors have shown great potential for clinical diagnostic applications due to their high sensitivity, specificity, and versatility; however, several challenges must be overcome for aptasensors to reach the clinical diagnostic test market, including 1) Standardization: There is a lack of standardization in the design, synthesis, and characterization of aptamers and aptasensors, which can affect their reproducibility and comparability. Standardization protocols need to be established to ensure the quality and reliability of aptasensors for clinical use; 2) Stability: Aptamers can undergo conformational changes under different conditions, such as changes in temperature, pH, and ionic strength,

which can affect their binding affinity and specificity. Strategies for stabilizing aptamers and aptasensors under different conditions need to be developed to ensure their robustness and long-term stability; 3) Sample complexity: Clinical samples, such as blood, urine, and saliva, are often complex and contain a variety of interfering substances that can affect the performance of aptasensors. Methods for sample preparation and purification need to be developed to minimize interference and enhance the sensitivity and specificity of aptasensors; 4) Cost-effectiveness: Aptasensors need to be cost-effective and scalable for mass production to be suitable for clinical use. The cost of aptamer synthesis and sensor fabrication needs to be reduced, and manufacturing processes need to be optimized to increase efficiency and reduce production costs; 5) Regulatory approval: Aptasensors need to undergo rigorous regulatory approval processes before they can be used in clinical settings. Safety, efficacy, and quality standards need to be established, and clinical trials need to be conducted to demonstrate their clinical utility and effectiveness; 6) Commercialization: Aptasensors need to be commercialized by companies with the necessary resources and expertise to market, distribute, and support them. The market demand for aptasensors needs to be assessed, and strategies for commercialization need to be developed to ensure their widespread adoption and sustainability.

Declaration of competing interest

The authors declare that they have no known competing financial interests or personal relationships that could have appeared to influence the work reported in this paper.

Data availability

No data was used for the research described in the article.

Acknowledgements

The authors acknowledge the financial support from São Paulo Research Foundation- FAPESP (processes 2019/27021-4, 2017/13137-5 and 2014/50867-3) and from to the National Council for Research-CNPq (processes 311847-2018-8 and 465389/2014-7).

References

[1] H.K. Matthews, C. Bertoli, R.A. de Bruin, Cell cycle control in cancer, Nat. Rev. Mol. Cell Biol. 23 (1) (2022) 74–88.
[2] I. Martínez-Reyes, N.S. Chandel, Cancer metabolism: looking forward, Nat. Rev. Cancer 21 (10) (2021) 669–680.
[3] F. Smith, Theory of Disease, Naturopathic Medicine, Springer, 2022, pp. 17–38.
[4] J. Ferlay, M. Colombet, I. Soerjomataram, D.M. Parkin, M. Piñeros, A. Znaor, F. Bray, Cancer statistics for the year 2020: an overview, Int. J. Cancer 149 (4) (2021) 778–789.
[5] D. Sarfati, J. Gurney, Preventing cancer: the only way forward, Lancet 400 (10352) (2022) 540–541.
[6] C. Ganini, I. Amelio, R. Bertolo, P. Bove, O.C. Buonomo, E. Candi, C. Cipriani, N. Di Daniele, H. Juhl, A. Mauriello, Global mapping of cancers: the cancer genome atlas and beyond, Mol. Oncol. 15 (11) (2021) 2823–2840.
[7] J. Javier-DesLoges, T.J. Nelson, J.D. Murphy, R.R. McKay, E. Pan, J.K. Parsons, C. J. Kane, A.K. Kader, I.H. Derweesh, J. Nodora, Disparities and trends in the participation of minorities, women, and the elderly in breast, colorectal, lung, and prostate cancer clinical trials, Cancer 128 (4) (2022) 770–777.
[8] I. Vitale, E. Shema, S. Loi, L. Galluzzi, Intratumoral heterogeneity in cancer progression and response to immunotherapy, Nat. Med. 27 (2) (2021) 212–224.
[9] W. Jiang, Y. Wang, J.A. Wargo, F.F. Lang, B. Kim, Considerations for designing preclinical cancer immune nanomedicine studies, Nat. Nanotechnol. 16 (1) (2021) 6–15.
[10] H. Xiaogang, M. Sharma, G. Ali, X. Li, E.-S. Salama, The role of nutrition in harnessing the immune system: a potential approach to prevent cancer, Med. Oncol. 39 (12) (2022) 1–17.
[11] C. Muresanu, S. Khalchitsky, Updated understanding of the causes of cancer, and a new theoretical perspective of combinational cancer therapies, a hypothesis, DNA Cell Biol. 41 (4) (2022) 342–355.
[12] R. Guan, Q. Van Le, H. Yang, D. Zhang, H. Gu, Y. Yang, C. Sonne, S.S. Lam, J. Zhong, Z. Jianguang, A review of dietary phytochemicals and their relation to oxidative stress and human diseases, Chemosphere 271 (2021), 129499.
[13] A. Seiler, M.A. Chen, R.L. Brown, C.P. Fagundes, Obesity, dietary factors, nutrition, and breast cancer risk, Curr. Breast Cancer Rep. 10 (1) (2018) 14–27.
[14] N. Menon, M. Mandelkern, Utility of PET scans in the diagnosis and management of gastrointestinal tumors, Dig. Dis. Sci. 67 (10) (2022) 4633–4653.
[15] E. Burian, B. Palla, N. Callahan, T. Pyka, C. Wolff, C.E. von Schacky, A. Schmid, M.F. Froelich, J. Rübenthaler, M.R. Makowski, Comparison of CT, MRI, and F-18 FDG PET/CT for initial N-staging of oral squamous cell carcinoma: a cost-effectiveness analysis, Eur. J. Nucl. Med. Mol. Imag. 49 (11) (2022) 3870–3877.
[16] T. Ariizumi, H. Kawashima, T. Yamagishi, N. Oike, Y. Murayama, H. Umezu, N. Endo, A. Ogose, Diagnostic accuracy of fine needle aspiration cytology and core needle biopsy in bone and soft tissue tumor: a comparative study of the image-guided and blindly performed procedure, Ann. Diagn. Pathol. 59 (2022), 151936.
[17] Z. Liu, W. Su, J. Ao, M. Wang, Q. Jiang, J. He, H. Gao, S. Lei, J. Nie, X. Yan, Instant diagnosis of gastroscopic biopsy via deep-learned single-shot femtosecond stimulated Raman histology, Nat. Commun. 13 (1) (2022) 4050.
[18] J.V. Hull, M.R. Padkins, S. El Hajj, M.A. Al-Hijji, A. Kanwar, D.J. Crusan, R. Gulati, A. El Sabbagh, J.Y. Park, R.J. Lennon, Risks of right heart catheterization and right ventricular biopsy: a 12-year, single-center experience, in: Mayo Clinic Proceedings, Elsevier, 2023, pp. 419–431.
[19] N.P. Chalasani, K. Porter, A. Bhattacharya, A.J. Book, B.M. Neis, K.M. Xiong, T. S. Ramasubramanian, I. Chen, S. Johnson, L.R. Roberts, Validation of a novel multitarget blood test shows high sensitivity to detect early stage hepatocellular carcinoma, Clin. Gastroenterol. Hepatol. 20 (1) (2022) 173–182. e7.
[20] X. Li, P. Gong, Q. Zhao, X. Zhou, Y. Zhang, Y. Zhao, Plug-in optical fiber SPR biosensor for lung cancer gene detection with temperature and pH compensation, Sensor. Actuator. B Chem. 359 (2022), 131596.
[21] J. Pascual, G. Attard, F.-C. Bidard, G. Curigliano, L. de Mattos-Arruda, M. Diehn, A. Italiano, J. Lindberg, J.D. Merker, C. Montagut, ESMO recommendations on the use of circulating tumour DNA assays for patients with cancer: a report from the ESMO Precision Medicine Working Group, Ann. Oncol. 33 (8) (2022) 750–768.
[22] N.P. Lee, N.S. Yee, Cancer Biomarkers and Targets in Digestive Organs, Mdpi AG, 2019.
[23] G.D. Dakubo, Cancer Biomarkers in Body Fluids: Biomarkers in Proximal Fluids, Springer International Publishing, 2019.
[24] M. Negahdary, N. Sattarahmady, H. Heli, Advances in prostate specific antigen biosensors-impact of nanotechnology, Clin. Chim. Acta 504 (2020) 43–55.
[25] H. Padinharayil, J. Varghese, M.C. John, G.K. Rajanikant, C.M. Wilson, M. Al-Yozbaki, K. Renu, S. Dewanjee, R. Sanyal, A. Dey, Non-small Cell Lung Carcinoma (NSCLC): Implications on Molecular Pathology and Advances in Early Diagnostics and Therapeutics, Genes & Diseases, 2022.
[26] S. Li, Q. Ma, Electrochemical nano-sensing interface for exosomes analysis and cancer diagnosis, Biosens. Bioelectron. 214 (2022), 114554.
[27] M. Negahdary, Aptamers in nanostructure-based electrochemical biosensors for cardiac biomarkers and cancer biomarkers: a review, Biosens. Bioelectron. 152 (2020), 112018.
[28] M. Negahdary, L. Angnes, Electrochemical aptamer-based nanobiosensors for diagnosing Alzheimer's disease: a review, Mater. Sci. Eng. C (2022), 112689.
[29] P. Singh, Electrochemical Biosensors: Applications in Diagnostics, Therapeutics, Environment, and Food Management, Elsevier Science, 2021.
[30] A. Azzouz, L. Hejji, C. Sonne, K.-H. Kim, V. Kumar, Nanomaterial-based aptasensors as an efficient substitute for cardiovascular disease diagnosis: future of smart biosensors, Biosens. Bioelectron. 193 (2021), 113617.
[31] M. Negahdary, Electrochemical aptasensors based on the gold nanostructures, Talanta 216 (2020), 120999.
[32] B. Mohan, S. Kumar, V. Kumar, T. Jiao, H.K. Sharma, Q. Chen, Electrochemiluminescence metal-organic frameworks biosensing materials for detecting cancer biomarkers, TrAC, Trends Anal. Chem. (2022), 116735.
[33] B. Kaur, S. Kumar, B.K. Kaushik, Recent advancements in optical biosensors for cancer detection, Biosens. Bioelectron. 197 (2022), 113805.
[34] A. Maleki, M. Ghomi, N. Nikfarjam, M. Akbari, E. Sharifi, M.A. Shahbazi, M. Kermanian, M. Seyedhamzeh, E. Nazarzadeh Zare, M. Mehrali, Biomedical applications of MXene-integrated composites: regenerative medicine, infection therapy, cancer treatment, and biosensing, Adv. Funct. Mater. 32 (34) (2022), 2203430.
[35] H. Mao, L. Yu, M. Tu, S. Wang, J. Zhao, H. Zhang, Y. Cao, Recent advances on the metal-organic frameworks-based biosensing methods for cancer biomarkers detection, Crit. Rev. Anal. Chem. (2022) 1–17.
[36] M. Heiat, M. Negahdary, Sensitive diagnosis of alpha-fetoprotein by a label free nanoaptasensor designed by modified Au electrode with spindle-shaped gold nanostructure, Microchem. J. 148 (2019) 456–466.
[37] A. Khanmohammadi, A. Aghaie, E. Vahedi, A. Qazvini, M. Ghanei, A. Afkhami, A. Hajian, H. Bagheri, Electrochemical biosensors for the detection of lung cancer biomarkers: a review, Talanta 206 (2020), 120251.
[38] S. Zhang, F. Rong, C. Guo, F. Duan, L. He, M. Wang, Z. Zhang, M. Kang, M. Du, Metal–organic frameworks (MOFs) based electrochemical biosensors for early cancer diagnosis in vitro, Coord. Chem. Rev. 439 (2021), 213948.
[39] J.C. Rosch, D.A. Balikov, F. Gong, E.S. Lippmann, A systematic evolution of ligands by exponential enrichment workflow with consolidated counterselection to efficiently isolate high-affinity aptamers, Eng. Rep. 2 (1) (2020), e12089.
[40] G. Kenguva, S.R. Rout, L. Giri, A. Sahebkar, P. Kesharwani, R. Dandela, Cell-SELEX Technology for Aptamer Selection, Aptamers Engineered Nanocarriers for Cancer Therapy, Elsevier, 2023, pp. 1–20.

[41] H. Yue, J. Chen, X. Chen, X. Wang, Y. Zhang, N. Zhou, Systematic screening and optimization of single-stranded DNA aptamer specific for N-acetylneuraminic acid: a comparative study, Sensor. Actuator. B Chem. 344 (2021), 130270.
[42] A. Bashir, Q. Yang, J. Wang, S. Hoyer, W. Chou, C. McLean, G. Davis, Q. Gong, Z. Armstrong, J. Jang, Machine learning guided aptamer refinement and discovery, Nat. Commun. 12 (1) (2021) 1–11.
[43] A. Atapour, H. Khajehzadeh, M. Shafie, M. Abbasi, S. Mosleh-Shirazi, S.R. Kasaee, A.M. Amani, Gold nanoparticle-based aptasensors: a promising perspective for early-stage detection of cancer biomarkers, Mater. Today Commun. (2022), 103181.
[44] S. Qi, N. Duan, I.M. Khan, X. Dong, Y. Zhang, S. Wu, Z. Wang, Strategies to manipulate the performance of aptamers in SELEX, post-SELEX and microenvironment, Biotechnol. Adv. (2022), 107902.
[45] S. Liu, Y. Xu, X. Jiang, H. Tan, B. Ying, Translation of aptamers toward clinical diagnosis and commercialization, Biosens. Bioelectron. (2022), 114168.
[46] R. Eivazzadeh-Keihan, P. Pashazadeh-Panahi, B. Baradaran, A. Maleki, M. Hejazi, A. Mokhtarzadeh, M. de la Guardia, Recent advances on nanomaterial based electrochemical and optical aptasensors for detection of cancer biomarkers, TrAC, Trends Anal. Chem. 100 (2018) 103–115.
[47] P. Malik, R. Gupta, V. Malik, R.K. Ameta, Emerging nanomaterials for improved biosensing, Measurement: Sensors 16 (2021), 100050.
[48] Y. Zhao, K. Yavari, J. Liu, Critical evaluation of aptamer binding for biosensor designs, TrAC, Trends Anal. Chem. 146 (2022), 116480.
[49] A. Wu, W.S. Khan, Nanobiosensors: from Design to Applications, Wiley, 2020.
[50] S. Su, Q. Sun, X. Gu, Y. Xu, J. Shen, D. Zhu, J. Chao, C. Fan, L. Wang, Two-dimensional nanomaterials for biosensing applications, TrAC, Trends Anal. Chem. 119 (2019), 115610.
[51] H. Kaur, M. Shorie, Nanomaterial based aptasensors for clinical and environmental diagnostic applications, Nanoscale Adv. 1 (6) (2019) 2123–2138.
[52] M. Falahati, F. Attar, M. Sharifi, A.A. Saboury, A. Salihi, F.M. Aziz, I. Kostova, C. Burda, P. Priecel, J.A. Lopez-Sanchez, Gold nanomaterials as key suppliers in biological and chemical sensing, catalysis, and medicine, Biochim. Biophys. Acta, Gen. Subj. 1864 (1) (2020), 129435.
[53] I. Saldan, O. Dobrovetska, L. Sus, O. Makota, O. Pereviznyk, O. Kuntyi, O. Reshetnyak, Electrochemical synthesis and properties of gold nanomaterials, J. Solid State Electrochem. 22 (3) (2018) 637–656.
[54] C. Sheng, J. Zhao, F. Yu, L. Li, Enzyme Translocation-Mediated Signal Amplification for Spatially Selective Aptasensing of ATP in Inflammatory Cells, Angew. Chem., Int. Ed. 62 (14) (2023), e202217551.
[55] C. Niu, X. Lin, X. Jiang, F. Guo, J. Liu, X. Liu, H. Huang, Y. Huang, An electrochemical aptasensor for highly sensitive detection of CEA based on exonuclease III and hybrid chain reaction dual signal amplification, Bioelectrochemistry 143 (2022), 107986.
[56] Y. Zhu, J. Wang, H. Xie, C. Fu, J. Zhou, H. Liu, P. Zeng, Y. Sun, Double signal amplification strategy for dual-analyte fluorescent aptasensors for visualizing cancer biomarker proteins, Anal. Chem. 94 (29) (2022) 10451–10461.
[57] A.B. Hashkavayi, B.S. Cha, E.S. Lee, K.S. Park, Dual rolling circle amplification-enabled ultrasensitive multiplex detection of exosome biomarkers using electrochemical aptasensors, Anal. Chim. Acta 1205 (2022), 339762.
[58] C. Li, M. Zhou, H. Wang, J. Wang, L. Huang, Rolling circle amplification assisted dual signal amplification colorimetric biosensor for ultrasensitive detection of leukemia-derived exosomes, Talanta 245 (2022), 123444.
[59] Y. Xu, N. Cheng, Y. Luo, K. Huang, Q. Chang, G. Pang, W. Xu, An Exo III-assisted catalytic hairpin assembly-based self-fluorescence aptasensor for pesticide detection, Sensor. Actuator. B Chem. 358 (2022), 131441.
[60] P. Yang, X. Guo, J. Zhang, C. Chen, Y. Gan, W. Xie, Y. Du, Z. Wu, Picomolar thrombin detection by orchestration of triple signal amplification strategy with hierarchically porous Ti3C2Tx MXene electrode material-catalytic hairpin assembly reaction-metallic nanoprobes, Biosens. Bioelectron. 208 (2022), 114228.
[61] U.S. Kadam, J.C. Hong, Recent advances in aptameric biosensors designed to detect toxic contaminants from food, water, human fluids, and the environment, Trend. Environ. Anal. Chem. (2022), e00184.
[62] R. Thevendran, M. Citartan, Assays to estimate the binding affinity of aptamers, Talanta 238 (2022), 122971.
[63] M.H. Umbehr, B. Gurel, T.J. Murtola, S. Sutcliffe, S.B. Peskoe, C.M. Tangen, P. J. Goodman, I.M. Thompson, S.M. Lippman, M.S. Lucia, Intraprostatic inflammation is positively associated with serum PSA in men with PSA< 4 ng ml− 1, normal DRE and negative for prostate cancer, Prostate Cancer Prostatic Dis. 18 (3) (2015) 264–269.
[64] S.V. Carlsson, K. Murata, D.C. Danila, H. Lilja, PSA: Role in Screening and Monitoring Patients with Prostate Cancer, Cancer Biomarkers, Elsevier, 2022, pp. 131–172.
[65] A.L. Magnussen, I.G. Mills, Prostate Cancer Biomarkers: the Old and the New, Biomarkers of the Tumor Microenvironment, Springer, 2022, pp. 467–482.
[66] A. Díaz-Fernández, R. Miranda-Castro, N. de-los-Santos-Álvarez, M.J. Lobo-Castañón, P. Estrela, Impedimetric aptamer-based glycan PSA score for discrimination of prostate cancer from other prostate diseases, Biosens. Bioelectron. 175 (2021), 112872.
[67] R. Xu, Y. Du, H. Ma, D. Wu, X. Ren, X. Sun, Q. Wei, H. Ju, Photoelectrochemical aptasensor based on La2Ti2O7/Sb2S3 and V2O5 for effectively signal change strategy for cancer marker detection, Biosens. Bioelectron. 192 (2021), 113528.
[68] N. Beauchemin, A. Arabzadeh, Carcinoembryonic antigen-related cell adhesion molecules (CEACAMs) in cancer progression and metastasis, Cancer Metastasis Rev. 32 (2013) 643–671.
[69] M.A. Haque, Glycoproteins and Cancer Biomarkers, Current Cancer Biomarkers, 2023, p. 195.
[70] S. Liu, D. Lin, Y. Lai, L. Hou, T. Lin, S. Zhao, Gas-Mediated Immunoassay for the Carcinoembryonic Antigen at Atmospheric Pressure with Smartphone Coupling with the Fluorescence Quenching Length of Perovskite Capillary, Anal. Chem. 94 (51) (2022) 18074–18082.
[71] M.C. Roşu, P.D. Mihnea, A. Ardelean, S.D. Moldovan, R.O. Popeţiu, B.D. Totolici, Clinical significance of tumor necrosis factor-alpha and carcinoembryonic antigen in gastric cancer, J. Med. Life 15 (1) (2022) 4.
[72] H. Khan, M.R. Shah, J. Barek, M.I. Malik, Cancer biomarkers and their biosensors: a comprehensive review, TrAC, Trends Anal. Chem. (2022), 116813.
[73] S.I. Kaya, G. Ozcelikay, F. Mollarasouli, N.K. Bakirhan, S.A. Ozkan, Recent achievements and challenges on nanomaterial based electrochemical biosensors for the detection of colon and lung cancer biomarkers, Sensor. Actuator. B Chem. 351 (2022), 130856.
[74] X. Song, H. Gao, R. Yuan, Y. Xiang, Trimetallic nanoparticle-decorated MXene nanosheets for catalytic electrochemical detection of carcinoembryonic antigen via Exo III-aided dual recycling amplifications, Sensor. Actuator. B Chem. 359 (2022), 131617.
[75] K.N. Seale, K.H. Tkaczuk, Circulating biomarkers in breast cancer, Clin. Breast Cancer 22 (3) (2022) e319–e331.
[76] G. Manasa, R.J. Mascarenhas, N.P. Shetti, S.J. Malode, T.M. Aminabhavi, Biomarkers for early diagnosis of ovarian carcinoma, ACS Biomater. Sci. Eng. 8 (7) (2022) 2726–2746.
[77] I.M. Mostafa, Y. Tian, S. Anjum, S. Hanif, M. Hosseini, B. Lou, G. Xu, Comprehensive review on the electrochemical biosensors of different breast cancer biomarkers, Sensor. Actuator. B Chem. (2022), 131944.
[78] F.-T. Xie, Y.-L. Li, Y. Guan, J.-W. Liu, T. Yang, G.-J. Mao, Y. Wu, Y.-H. Yang, R. Hu, Ultrasensitive dual-signal electrochemical ratiometric aptasensor based on Co-MOFs with intrinsic self-calibration property for Mucin 1, Anal. Chim. Acta 1225 (2022), 340219.
[79] H. Zhao, T. Liu, L. Cui, Y. Li, F. Yang, X. Zhang, Label-free and dual-amplified electrochemical bioanalysis of MUC1 based on an inorganic-organic polymer hybrid mimic peroxidase (AuNPs@Cu7S4@Cu/Mn-AzoPPOP) and catalytic hairpin assembly, Sensor. Actuator. B Chem. 345 (2021), 130332.
[80] F. Liu, L. Geng, F. Ye, S. Zhao, MOF-derived MnO@C nanocomposite with bidirectional electrocatalytic ability as signal amplification for dual-signal electrochemical sensing of cancer biomarker, Talanta 239 (2022), 123150.
[81] L.L. Wu, C.-C. Chiou, P.-Y. Chang, J.T. Wu, Urinary 8-OHdG: a marker of oxidative stress to DNA and a risk factor for cancer, atherosclerosis and diabetics, Clin. Chim. Acta 339 (1) (2004) 1–9.
[82] M.-P. Martinez-Moral, K. Kannan, Analysis of 19 urinary biomarkers of oxidative stress, nitrative stress, metabolic disorders, and inflammation using liquid chromatography–tandem mass spectrometry, Anal. Bioanal. Chem. 414 (6) (2022) 2103–2116.
[83] Y. Geng, M. Hu, Y. Yao, M. Zhan, Y. Zhou, Urinary concentrations of amphenicol antibiotics in relation to biomarkers of oxidative DNA and RNA damage in school children, J. Environ. Sci. Health, Part A (2022) 1–9.
[84] J. Xu, J. Zhang, R. Zeng, L. Li, M. Li, D. Tang, Target-induced photocurrent-polarity-switching photoelectrochemical aptasensor with gold nanoparticle-ZnIn2S4 nanohybrids for the quantification of 8-hydroxy-2′-deoxyguanosine, Sensor. Actuator. B Chem. 368 (2022), 132141.
[85] L. Keller, S. Werner, K. Pantel, Biology and clinical relevance of EpCAM, Cell Stress 3 (6) (2019) 165.
[86] O. Gires, M. Pan, H. Schinke, M. Canis, P.A. Baeuerle, Expression and function of epithelial cell adhesion molecule EpCAM: where are we after 40 years? Cancer Metastasis Rev. 39 (2020) 969–987.
[87] A. Herreros-Pomares, C. Aguilar-Gallardo, S. Calabuig-Fariñas, R. Sirera, E. Jantus-Lewintre, C. Camps, EpCAM duality becomes this molecule in a new Dr. Jekyll and Mr. Hyde tale, Crit. Rev. Oncol. Hematol. 126 (2018) 52–63.
[88] M. Munz, P.A. Baeuerle, O. Gires, The emerging role of EpCAM in cancer and stem cell signaling, Cancer Res. 69 (14) (2009) 5627–5629.
[89] U. Schnell, V. Cirulli, B.N. Giepmans, EpCAM: structure and function in health and disease, Biochim. Biophys. Acta, Biomembr. 1828 (8) (2013) 1989–2001.
[90] M.-E. Goebeler, R.C. Bargou, T cell-engaging therapies—BiTEs and beyond, Nat. Rev. Clin. Oncol. 17 (7) (2020) 418–434.
[91] D. Barkley, R. Moncada, M. Pour, D.A. Liberman, I. Dryg, G. Werba, W. Wang, M. Baron, A. Rao, B. Xia, Cancer cell states recur across tumor types and form specific interactions with the tumor microenvironment, Nat. Genet. 54 (8) (2022) 1192–1201.
[92] X. Wang, L. Tian, J. Lu, I.O.-L. Ng, Exosomes and cancer-Diagnostic and prognostic biomarkers and therapeutic vehicle, Oncogenesis 11 (1) (2022) 1–12.
[93] Y. Zhao, J. Yao, Z. Wu, H. Liu, W. Zheng, AuPt NPs with enhanced electrochemical oxidization activity for ratiometric electrochemical aptasensor, Biosens. Bioelectron. 196 (2022), 113733.
[94] A. Bagheri Hashkavayi, B.S. Cha, S.H. Hwang, J. Kim, K.S. Park, Highly sensitive electrochemical detection of circulating EpCAM-positive tumor cells using a dual signal amplification strategy, Sensor. Actuator. B Chem. 343 (2021), 130087.
[95] E. Alspach, D.M. Lussier, R.D. Schreiber, Interferon γ and its important roles in promoting and inhibiting spontaneous and therapeutic cancer immunity, Cold Spring Harbor Perspect. Biol. 11 (3) (2019) a028480.
[96] A.T. Mostafa, A.A. Abd Allah, R. Hafez, S. Hussien, R.M. Bakry, Interleukin-4, and interferon-gamma roles as biomarkers in Systemic Lupus Erythematosus patients, Sohag Med. J. 26 (1) (2022) 51–59.
[97] B.E. Lippitz, Cytokine patterns in patients with cancer: a systematic review, Lancet Oncol. 14 (6) (2013) e218–e228.

[98] A.M. Gocher, C.J. Workman, D.A. Vignali, Interferon-γ: teammate or opponent in the tumour microenvironment? Nat. Rev. Immunol. 22 (3) (2022) 158–172.
[99] P.-C. Tseng, C.-L. Chen, K.-Y. Lee, P.-H. Feng, Y.-C. Wang, R.D. Satria, C.-F. Lin, Epithelial-to-mesenchymal transition hinders interferon-γ-dependent immunosurveillance in lung cancer cells, Cancer Lett. 539 (2022), 215712.
[100] E.R. Abt, T.M. Le, A.M. Dann, J.R. Capri, S. Poddar, V. Lok, L. Li, K. Liang, A. L. Creech, K. Rashid, Reprogramming of nucleotide metabolism by interferon confers dependence on the replication stress response pathway in pancreatic cancer cells, Cell Rep. 38 (2) (2022), 110236.
[101] Y. Zhou, J. Liu, H. Dong, Z. Liu, L. Wang, Q. Li, J. Ren, Y. Zhang, M. Xu, Target-induced silver nanocluster generation for highly sensitive electrochemical aptasensor towards cell-secreted interferon-γ, Biosens. Bioelectron. 203 (2022), 114042.
[102] X. Tang, C. Lu, X. Xu, Z. Ding, H. Li, H. Zhang, Y. Wang, C. Li, A visible and near-infrared light dual responsive "signal-off" and "signal-on" photoelectrochemical aptasensor for prostate-specific antigen, Biosens. Bioelectron. 202 (2022), 113905.
[103] S.R. Nxele, R. Nkhahle, T. Nyokong, The synergistic effects of coupling Au nanoparticles with an alkynyl Co(II) phthalocyanine on the detection of prostate specific antigen, Talanta 237 (2022), 122948.
[104] P. Wang, H. Ma, Y. Zhu, W. Feng, M. Su, S. Li, H. Mao, A new ratiometric electrochemical aptasensor for the sensitive detection of carcinoembryonic antigen based on exonuclease I-assisted target recycling and hybridization chain reaction amplification strategy, J. Electroanal. Chem. 910 (2022), 116167.
[105] H. Ma, P. Wang, Y. Xie, J. Liu, W. Feng, S. Li, Ratiometric electrochemical aptasensor for the sensitive detection of carcinoembryonic antigen based on a hairpin DNA probe and exonuclease I-assisted target recycling, Anal. Biochem. 649 (2022), 114694.
[106] X. Wang, R. Chen, J. Hu, W. Yuan, An adjustable amyloid-β oligomers aptasensor based on the synergistic effect of self-enhanced metal-organic gel luminophore and triple-helix DNA system, Int. J. Biol. Macromol. 222 (2022) 794–802.
[107] Z.Y. Li, D.Y. Li, L. Huang, R. Hu, T. Yang, Y.H. Yang, An electrochemical aptasensor based on intelligent walking DNA nanomachine with cascade signal amplification powered by nuclease for Mucin 1 assay, Anal. Chim. Acta 1214 (2022), 339964.
[108] C. Zhao, W. Guo, A. Umar, H. Algadi, M. Pei, A.A. Ibrahim, X. Yang, Z. Ren, X. Mi, L. Wang, High-sensitive ferrocene labeled aptasensor for the detection of Mucin 1 by tuning the sequence constitution of complementary probe, Microchim. Acta 189 (9) (2022) 332.
[109] A. Khoshroo, A. Fattahi, L. Hosseinzadeh, Development of paper-based aptasensor for circulating tumor cells detection in the breast cancer, J. Electroanal. Chem. 910 (2022), 116182.
[110] N. Xia, D. Wu, H. Yu, W. Sun, X. Yi, L. Liu, Magnetic bead-based electrochemical and colorimetric assays of circulating tumor cells with boronic acid derivatives as the recognition elements and signal probes, Talanta 221 (2021), 121640.
[111] W. Yang, L. Fan, Z. Guo, H. Wu, J. Chen, C. Liu, Y. Yan, S. Ding, Reversible capturing and voltammetric determination of circulating tumor cells using two-dimensional nanozyme based on PdMo decorated with gold nanoparticles and aptamer, Microchim. Acta 188 (10) (2021) 319.
[112] Z.O. Uygun, F.G. Sağin, Detection of circulating prostate cancer cells via prostate specific membrane antigen by chronoimpedimetric aptasensor, Turk. J. Biochem. 46 (6) (2021) 631–637.
[113] Q. Liu, X. Yue, Y. Li, F. Wu, M. Meng, Y. Yin, R. Xi, A novel electrochemical aptasensor for exosomes determination and release based on specific host-guest interactions between cucurbit [7]uril and ferrocene, Talanta 232 (2021), 122451.
[114] M. Chen, R. Han, W. Wang, Y. Li, X. Luo, Antifouling aptasensor based on self-assembled loop-closed peptides with enhanced stability for CA125 assay in complex biofluids, Anal. Chem. 93 (40) (2021) 13555–13563.
[115] X. He, X. Wang, C. Ge, S. Li, L. Wang, Y. Xu, Detection of VEGF165 in whole blood by differential pulse voltammetry based on a centrifugal microfluidic chip, ACS Sens. 7 (4) (2022) 1019–1026.
[116] C. Lin, Q. Huang, X. Hong, S. Hong, X. Shu, E. Wang, L. Wang, W. Fu, Z. Lin, Electrochemiluminescence aptasensor for vascular endothelial growth factor 165 detection based on Ru(bpy)32+/Au nanoparticles film modified electrode and double signal amplification, Bioelectrochemistry 146 (2022), 108151.
[117] Y. Zhang, M. Liu, S. Pan, L. Yu, S. Zhang, R. Liu, A magnetically induced self-assembled and label-free electrochemical aptasensor based on magnetic Fe3O4/Fe2O3@Au nanoparticles for VEGF165 protein detection, Appl. Surf. Sci. 580 (2022), 152362.
[118] Y. Huang, X. Pei, S. Du, Z. Li, X. Gu, W. Sun, X. Niu, Target-induced ratiometric electrochemical aptasensor for highly sensitive detection of thrombin based on AuNPs-MXene, Microchem. J. 181 (2022), 107774.
[119] C. Erkmen, G.A. Tığ, B. Uslu, Nanomaterial-based sandwich-type electrochemical aptasensor platform for sensitive voltammetric determination of leptin, Microchim. Acta 189 (10) (2022) 396.
[120] J. Quan, Y. Wang, J. Zhang, K. Huang, X. Wang, H. Jiang, Aptamer embedded arch-cruciform DNA assemblies on 2-D VS2 scaffolds for sensitive detection of breast cancer cells, Biosensors 11 (10) (2021) 378.
[121] X. Xu, Z. Ding, X. Zhang, R. Zha, W. Li, L. Xu, D. Sun, X. Cai, T. Liang, Y. Wang, C. Li, A near-infrared photoelectrochemical aptasensing system based on Bi2O2S nanoflowers and gold nanoparticles for high-performance determination of MCF-7 cells, Anal. Chim. Acta 1251 (2023), 340982.
[122] X. Zhang, H. Li, W. Li, H. Liang, Z. Ding, L. Xu, Y. Zhang, X. Xu, C. Li, H. Li, Y. Wang, High-performance assaying phosphatidylinositol proteoglycan 3 based on a dual-mode biosensor coupling near-infrared photoelectrochemical with ratiometric electrochemical sensing, Sensor. Actuator. B Chem. 381 (2023), 133419.
[123] Y. Zhang, H. Ouyang, S. Zhang, Y. Ni, Z. Zhu, C. Ling, A. He, R. Liu, Label-free electrochemical bioplatform based on Au-modified magnetic Fe3O4/α-Fe2O3 hetero-nanorods for sensitive quantification of ovarian cancer tumor marker, Microchem. J. 189 (2023), 108546.
[124] R. Husna, C.P. Kurup, M.A. Ansari, N.F. Mohd-Naim, M.U. Ahmed, An electrochemical aptasensor based on AuNRs/AuNWs for sensitive detection of apolipoprotein A-1 (ApoA1) from human serum, RSC Adv. 13 (6) (2023) 3890–3898.
[125] G. Zhang, Z. Liu, L. Fan, Y. Han, Y. Guo, A novel dual signal and label-free electrochemical aptasensor for mucin 1 based on hemin/graphene@PdPtNPs, Biosens. Bioelectron. 173 (2021), 112785.
[126] J. Li, L. Zhao, W. Wang, Y. Liu, H. Yang, J. Kong, F. Si, Polymer-functionalized carbon nanotubes prepared via ring-opening polymerization for electrochemical detection of carcinoembryonic antigen, Sensor. Actuator. B Chem. 328 (2021), 129031.
[127] Z. Shen, S. Ni, W. Yang, W. Sun, G. Yang, G. Liu, Redox probes tagged electrochemical aptasensing device for simultaneous detection of multiple cytokines in real time, Sensor. Actuator. B Chem. 336 (2021), 129747.
[128] S. Robin Nxele, R. Nkhahle, T. Nyokong, The composites of asymmetric Co phthalocyanines-graphitic carbon nitride quantum dots-aptamer as specific electrochemical sensors for the detection of prostate specific antigen: effects of ring substituents, J. Electroanal. Chem. 900 (2021), 115730.
[129] S.R. Nxele, T. Nyokong, The effects of the composition and structure of quantum dots combined with cobalt phthalocyanine and an aptamer on the electrochemical detection of prostate specific antigen, Dyes Pigments 192 (2021), 109407.
[130] S.R. Nxele, T. Nyokong, The electrochemical detection of prostate specific antigen on glassy carbon electrode modified with combinations of graphene quantum dots, cobalt phthalocyanine and an aptamer, J. Inorg. Biochem. 221 (2021), 111462.
[131] F. Zhang, Z. Liu, Y. Han, L. Fan, Y. Guo, Sandwich electrochemical carcinoembryonic antigen aptasensor based on signal amplification of polydopamine functionalized graphene conjugate Pd-Pt nanodendrites, Bioelectrochemistry 142 (2021), 107947.
[132] P. Zhao, J. Zheng, Y. Liang, F. Tian, L. Peng, D. Huo, C. Hou, Functionalized carbon nanotube-decorated MXene nanosheet-enabled microfluidic electrochemical aptasensor for carcinoembryonic antigen determination, ACS Sustain. Chem. Eng. 9 (46) (2021) 15386–15393.
[133] R. Ma, S.C.B. Gopinath, T. Lakshmipriya, Y. Chen, Carbon material hybrid construction on an aptasensor for monitoring surgical tumors, J. Anal. Method. Chem. 2022 (2022), 9740784.
[134] M. Sadeghi, S. Kashanian, S.M. Naghib, E. Askari, F. Haghiralsadat, D. Tofighi, A highly sensitive nanobiosensor based on aptamer-conjugated graphene-decorated rhodium nanoparticles for detection of HER2-positive circulating tumor cells, Nanotechnol. Rev. 11 (1) (2022) 793–810.
[135] M. Sadeghi, S. Kashanian, S.M. Naghib, E. Arkan, A high-performance electrochemical aptasensor based on graphene-decorated rhodium nanoparticles to detect HER2-ECD oncomarker in liquid biopsy, Sci. Rep. 12 (1) (2022) 3299.
[136] M. Sadeghi, S. Kashanian, S.M. Naghib, F. Haghiralsadat, D. Tofighi, An efficient electrochemical biosensor based on pencil graphite electrode mediated by 2D functionalized graphene oxide to detect HER2 breast cancer biomarker, Int. J. Electrochem. Sci. 17 (220459) (2022) 2.
[137] S. Centane, T. Nyokong, Impedimetric aptasensor for HER2 biomarker using graphene quantum dots, polypyrrole and cobalt phthalocyanine modified electrodes, Sens. Bio-Sens. Res. 34 (2021), 100467.
[138] A.G. Crevillen, C.C. Mayorga-Martinez, J. Zelenka, S. Rimpelová, T. Ruml, M. Pumera, 3D-printed transmembrane glycoprotein cancer biomarker aptasensor, Appl. Mater. Today 24 (2021), 101153.
[139] Y. Park, M.-S. Hong, W.-H. Lee, J.-G. Kim, K. Kim, Highly sensitive electrochemical aptasensor for detecting the VEGF165 tumor marker with PANI/CNT nanocomposites, Biosensors 11 (4) (2021) 114.
[140] F. Zhang, L. Fan, Z. Liu, Y. Han, Y. Guo, A label-free electrochemical aptasensor for the detection of cancer antigen 125 based on nickel hexacyanoferrate nanocubes/polydopamine functionalized graphene, J. Electroanal. Chem. 918 (2022), 116424.
[141] A. Foroozandeh, M. Abdouss, H. SalarAmoli, M. Pourmadadi, F. Yazdian, An electrochemical aptasensor based on g-C3N4/Fe3O4/PANI nanocomposite applying cancer antigen_125 biomarkers detection, Process Biochem. 127 (2023) 82–91.
[142] S. Forouzanfar, I. Khakpour, F. Alam, N. Pala, C. Wang, Novel application of electrochemical bipolar exfoliated graphene for highly sensitive disposable label-free cancer biomarker aptasensors, Nanoscale Adv. 3 (20) (2021) 5948–5958.
[143] V. Mishyn, M. Aslan, A. Hugo, T. Rodrigues, H. Happy, R. Sanyal, W. Knoll, F. Baudoux, V. Bouchiat, R.O. Bilyy, R. Boukherroub, A. Sanyal, S. Szunerits, Catch and release strategy of matrix metalloprotease aptamers via thiol–disulfide exchange reaction on a graphene based electrochemical sensor, Sens. Diagnost. 1 (4) (2022) 739–749.
[144] Y. Tian, B. Wang, J. Wang, Q. Guo, X. Yang, G. Nie, A separated type cathode photoelectrochemical aptasensor for thrombin detection based on novel organic polymer heterojunction photoelectric material, Microchem. J. 175 (2022), 107140.
[145] K. Park, Impedance technique-based label-free electrochemical aptasensor for thrombin using single-walled carbon nanotubes-casted screen-printed carbon electrode, Sensors 22 (7) (2022) 2699.

[146] M. Qing, Z. Sun, L. Wang, S.Z. Du, J. Zhou, Q. Tang, H.Q. Luo, N.B. Li, CRISPR/Cas12a-regulated homogeneous electrochemical aptasensor for amplified detection of protein, Sensor. Actuator. B Chem. 348 (2021), 130713.
[147] S. Forouzanfar, N. Pala, C. Wang, In-Situ integration of 3D C-MEMS microelectrodes with bipolar exfoliated graphene for label-free electrochemical cancer biomarkers aptasensor, Micromachines 13 (1) (2022) 104.
[148] Z. Rahmati, M. Roushani, H. Hosseini, Hierarchical nickel hydroxide nanosheets grown on hollow nitrogen doped carbon nanoboxes as a high-performance surface substrate for alpha-fetoprotein cancer biomarkers electrochemical aptasensing, Talanta 237 (2022), 122924.
[149] R. Rawat, S. Singh, S. Roy, A. Kumar, T. Goswami, A. Mathur, Design and development of an electroanalytical genosensor based on Cu-PTCA/rGO nanocomposites for the detection of cervical cancer, Mater. Chem. Phys. 295 (2023), 127050.
[150] A. Rindiarti, Y. Okamoto, S. Nakagawa, J. Hirose, Y. Kodama, T. Nishikawa, Y. Kawano, Changes in intracellular activation-related gene expression and induction of Akt contribute to acquired resistance toward nelarabine in CCRF-CEM cell line, Leuk. Lymphoma 63 (2) (2022) 404–415.
[151] A. Khoshroo, L. Hosseinzadeh, K. Adib, M. Rahimi-Nasrabadi, F. Ahmadi, Earlier diagnoses of acute leukemia by a sandwich type of electrochemical aptasensor based on copper sulfide-graphene composite, Anal. Chim. Acta 1146 (2021) 1–10.
[152] M. Logozzi, D. Mizzoni, R. Di Raimo, S. Fais, Exosomes: a source for new and old biomarkers in cancer, Cancers 12 (9) (2020) 2566.
[153] K. Qian, W. Fu, T. Li, J. Zhao, C. Lei, S. Hu, The roles of small extracellular vesicles in cancer and immune regulation and translational potential in cancer therapy, J. Exp. Clin. Cancer Res. 41 (1) (2022) 1–29.
[154] S. Gupta, P. Mazumder, Exosomes as diagnostic tools, Adv. Clin. Chem. 110 (2022) 117–144.
[155] Y. Guo, S. Liu, H. Yang, P. Wang, Q. Feng, Regenerable electrochemical biosensor for exosomes detection based on the dual-recognition proximity binding-induced DNA walker, Sensor. Actuator. B Chem. 349 (2021), 130765.
[156] Z. Shekari, H.R. Zare, A. Falahati, Dual assaying of breast cancer biomarkers by using a sandwich–type electrochemical aptasensor based on a gold nanoparticles–3D graphene hydrogel nanocomposite and redox probes labeled aptamers, Sensor. Actuator. B Chem. 332 (2021), 129515.
[157] G. Mehdipour, J. Shabani Shayeh, M. Omidi, M. Pour Madadi, F. Yazdian, L. Tayebi, An electrochemical aptasensor for detection of prostate-specific antigen using reduced graphene gold nanocomposite and Cu/carbon quantum dots, Biotechnol. Appl. Biochem. 69 (5) (2022) 2102–2111.
[158] M. Pourmadadi, A. Nouralishahi, M. Shalbaf, J. Shabani Shayeh, A. Nouralishahi, An electrochemical aptasensor for detection of prostate-specific antigen-based on carbon quantum dots-gold nanoparticles, Biotechnol. Appl. Biochem. 70 (1) (2023) 175–183.
[159] S. Centane, T. Nyokong, Aptamer versus antibody as probes for the impedimetric biosensor for human epidermal growth factor receptor, J. Inorg. Biochem. 230 (2022), 111764.
[160] S. Centane, T. Nyokong, Co phthalocyanine mediated electrochemical detection of the HER2 in the presence of Au and CeO2 nanoparticles and graphene quantum dots, Bioelectrochemistry 149 (2023), 108301.
[161] A. Al Fatease, W. Guo, A. Umar, C. Zhao, Y. Alhamhoom, A.B. Muhsinah, M. H. Mahnashi, Z.A. Ansari, A dual-mode electrochemical aptasensor for the detection of Mucin-1 based on AuNPs-magnetic graphene composite, Microchem. J. 180 (2022), 107559.
[162] Z. Li, H. Li, X. Geng, G. Dai, Z. Chu, F. Luo, F. Zhang, Q. Wang, Sandwich-type electrochemical sensor for mucin-1 detection based on a cysteine–histidine–Cu@cuprous oxide nanozyme, ACS Appl. Nano Mater. 5 (2) (2022) 2204–2213.
[163] T. Ming, Y. Cheng, Y. Xing, J. Luo, G. Mao, J. Liu, S. Sun, F. Kong, H. Jin, X. Cai, Electrochemical microfluidic paper-based aptasensor platform based on a biotin–streptavidin system for label-free detection of biomarkers, ACS Appl. Mater. Interfaces 13 (39) (2021) 46317–46324.
[164] G. Li, H. Feng, X. Shi, M. Chen, J. Liang, Z. Zhou, Highly sensitive electrochemical aptasensor for Glypican-3 based on reduced graphene oxide-hemin nanocomposites modified on screen-printed electrode surface, Bioelectrochemistry 138 (2021), 107696.
[165] G. Li, B. Wang, L. Zhao, X. Shi, G. Wu, W. Chen, L. Sun, J. Liang, Z. Zhou, Label-free detection of glypican-3 using reduced graphene oxide/polyetherimide/gold nanoparticles enhanced aptamer specific sensing interface on light-addressable potentiometric sensor, Electrochim. Acta 426 (2022), 140808.
[166] Y. Xing, J. Liu, S. Sun, T. Ming, Y. Wang, J. Luo, G. Xiao, X. Li, J. Xie, X. Cai, New electrochemical method for programmed death-ligand 1 detection based on a paper-based microfluidic aptasensor, Bioelectrochemistry 140 (2021), 107789.
[167] F. Shafiei, R.S. Saberi, M.A. Mehrgardi, A label-free electrochemical aptasensor for breast cancer cell detection based on a reduced graphene oxide-chitosan-gold nanoparticle composite, Bioelectrochemistry 140 (2021), 107807.
[168] G. Li, M. Chen, B. Wang, C. Wang, G. Wu, J. Liang, Z. Zhou, Dual-signal sandwich-type aptasensor based on H-rGO-Mn3O4 nanozymes for ultrasensitive Golgi protein 73 determination, Anal. Chim. Acta 1221 (2022), 340102.
[169] L. Li, R. He, H. Yan, Z. Leng, S. Zhu, Z. Gu, Nanotechnology for the diagnosis and treatment of Alzheimer's disease: a bibliometric analysis, Nano Today 47 (2022), 101654.
[170] X.-J. Zhai, Q.-L. Wang, H.-F. Cui, X. Song, Q.-Y. Lv, Y. Guo, A DNAzyme-catalyzed label-free aptasensor based on multifunctional dendrimer-like DNA assembly for sensitive detection of carcinoembryonic antigen, Biosens. Bioelectron. 194 (2021), 113618.
[171] T. Inai, M. Mancuso, H. Hashizume, F. Baffert, A. Haskell, P. Baluk, D.D. Hu-Lowe, D.R. Shalinsky, G. Thurston, G.D. Yancopoulos, Inhibition of vascular endothelial growth factor (VEGF) signaling in cancer causes loss of endothelial fenestrations, regression of tumor vessels, and appearance of basement membrane ghosts, Am. J. Pathol. 165 (1) (2004) 35–52.
[172] S. Tunçer, R. Gurbanov, A novel approach for the discrimination of culture medium from Vascular Endothelial Growth Factor (VEGF) overexpressing colorectal cancer cells, Turk. J. Biochem. 45 (6) (2020) 715–724.
[173] X. Wang, J. Huang, W. Chen, G. Li, Z. Li, J. Lei, The updated role of exosomal proteins in the diagnosis, prognosis, and treatment of cancer, Exp. Mol. Med. (2022) 1–11.
[174] S.O. Alhaj-Suliman, E.I. Wafa, A.K. Salem, Engineering nanosystems to overcome barriers to cancer diagnosis and treatment, Adv. Drug Deliv. Rev. (2022), 114482.
[175] C. Mei, L. Pan, W. Xu, H. Xu, Y. Zhang, Z. Li, B. Dong, X. Ke, C. McAlinden, M. Yang, Q. Wang, J. Huang, An ultrasensitive reusable aptasensor for noninvasive diabetic retinopathy diagnosis target on tear biomarker, Sensor. Actuator. B Chem. 345 (2021), 130398.
[176] S. Zhang, H. Zheng, R. Jiang, J. Yuan, F. Li, T. Qin, A. Sakthivel, X. Liu, S. Alwarappan, Ultrasensitive PEC aptasensor based on one dimensional hierarchical SnS2|oxygen vacancy-WO3 co-sensitized by formation of a cascade structure for signal amplification, Sensor. Actuator. B Chem. 351 (2022), 130966.
[177] L. Wang, L. Zeng, Y. Wang, T. Chen, W. Chen, G. Chen, C. Li, J. Chen, Electrochemical aptasensor based on multidirectional hybridization chain reaction for detection of tumorous exosomes, Sensor. Actuator. B Chem. 332 (2021), 129471.
[178] R. Yan, N. Lu, S. Han, Z. Lu, Y. Xiao, Z. Zhao, M. Zhang, Simultaneous detection of dual biomarkers using hierarchical MoS2 nanostructuring and nano-signal amplification-based electrochemical aptasensor toward accurate diagnosis of prostate cancer, Biosens. Bioelectron. 197 (2022), 113797.
[179] J. Yao, J. Shao, H. Liu, Z. Wu, W. Zheng, H. Miao, Y. Zhao, Dual electroactive AgM (M=Ru, Pt) NPs for double electroanalysis of HER2 and EpCAM, Sensor. Actuator. B Chem. 357 (2022), 131436.
[180] Y. Song, K. Chen, S. Li, L. He, M. Wang, N. Zhou, M. Du, Impedimetric aptasensor based on zirconium–cobalt metal–organic framework for detection of carcinoembryonic antigen, Microchim. Acta 189 (9) (2022) 338.
[181] Y. Ji, J. Guo, B. Ye, G. Peng, C. Zhang, L. Zou, An ultrasensitive carcinoembryonic antigen electrochemical aptasensor based on 3D DNA nanoprobe and Exo III, Biosens. Bioelectron. 196 (2022), 113741.
[182] K. Zhang, M. Pei, Y. Cheng, Z. Zhang, C. Niu, X. Liu, J. Liu, F. Guo, H. Huang, X. Lin, A novel electrochemical aptamer biosensor based on tetrahedral DNA nanostructures and catalytic hairpin assembly for CEA detection, J. Electroanal. Chem. 898 (2021), 115635.
[183] S. Chen, S. Lin, X. Han, X. Han, Handheld pH-Meter-based electrochemical aptasensing of carcinoembryonic antigen on multifuctional magnetic beads, Electroanalysis 34 (10) (2022) 1547–1554.
[184] L. Shang, B.-J. Shi, W. Zhang, L.-P. Jia, R.-N. Ma, Q.-W. Xue, H.-S. Wang, W. Yan, Electrochemical stripping chemiluminescence coupled with recycling amplification strategy for sensitive detection of carcinoembryonic antigen, Sensor. Actuator. B Chem. 368 (2022), 132191.
[185] F.-F. Xin, Y. Xue, B.-F. Xu, A.-J. Wang, P. Song, L.-P. Mei, J.-J. Feng, Ultrasensitive "on-off-on" photoelectrochemical aptasensor for tumor biomarker using BiOI/α-Fe2O3 p-n heterojunction arrays by in-situ regulation of electron donor distance, Sensor. Actuator. B Chem. 375 (2023), 132933.
[186] S. Centane, S. Mgidlana, Y. Openda, T. Nyokong, Electrochemical detection of human epidermal growth factor receptor 2 using an aptamer on cobalt phthalocyanines – cerium oxide nanoparticle conjugate, Bioelectrochemistry 146 (2022), 108146.
[187] Y. Xu, Y. Zhang, N. Li, M. Yang, T. Xiang, D. Huo, Z. Qiu, L. Yang, C. Hou, An ultra-sensitive dual-signal ratiometric electrochemical aptasensor based on functionalized MOFs for detection of HER2, Bioelectrochemistry 148 (2022), 108272.
[188] F. Vajhadin, M. Mazloum-Ardakani, M. Shahidi, S.M. Moshtaghioun, F. Haghiralsadat, A. Ebadi, A. Amini, MXene-based cytosensor for the detection of HER2-positive cancer cells using CoFe2O4@Ag magnetic nanohybrids conjugated to the HB5 aptamer, Biosens. Bioelectron. 195 (2022), 113626.
[189] Y. Zhang, N. Li, Y. Xu, P. Lu, N. Qi, M. Yang, C. Hou, D. Huo, An ultrasensitive dual-signal aptasensor based on functionalized Sb@ZIF-67 nanocomposites for simultaneously detect multiple biomarkers, Biosens. Bioelectron. (2022), 114508.
[190] R. Li, Y. An, T. Jin, F. Zhang, P. He, Detection of MUC1 protein on tumor cells and their derived exosomes for breast cancer surveillance with an electrochemiluminescence aptasensor, J. Electroanal. Chem. 882 (2021), 115011.
[191] X. Liu, X. Gao, L. Yang, Y. Zhao, F. Li, Metal–organic framework-functionalized paper-based electrochemical biosensor for ultrasensitive exosome assay, Anal. Chem. 93 (34) (2021) 11792–11799.
[192] Y. Xia, T. Chen, W. Chen, G. Chen, L. Xu, L. Zhang, X. Zhang, W. Sun, J. Lan, X. Lin, J. Chen, A dual-modal aptasensor based on a multifunctional acridone derivate for exosomes detection, Anal. Chim. Acta 1191 (2022), 339279.
[193] J. Li, Y. Liu, C. Wang, Q. Jia, G. Zhang, X. Huang, N. Zhou, Z. Zhang, Determination of VEGF165 using impedimetric aptasensor based on cyclohexanehexone-melem covalent-organic framework, Microchim. Acta 188 (6) (2021) 211.
[194] C. Mei, Y. Zhang, L. Pan, B. Dong, X. Chen, Q. Gao, H. Xu, W. Xu, H. Fang, S. Liu, C. McAlinden, E.I. Paschalis, Q. Wang, M. Yang, J. Huang, A.-Y. Yu, A one-step electrochemical aptasensor based on signal amplification of metallo nanoenzyme particles for vascular endothelial growth factor, Front. Bioeng. Biotechnol. 10 (2022).
[195] J. Zhang, Y. Gao, X. Zhang, Q. Feng, C. Zhan, J. Song, W. Zhang, W. Song, "Dual signal-on" split-type aptasensor for TNF-α: integrating MQDs/ZIF-8@ZnO NR

arrays with MB-liposome-mediated signal amplification, Anal. Chem. 93 (19) (2021) 7242–7249.
[196] Y. Ni, H. Ouyang, L. Yu, C. Ling, Z. Zhu, A. He, R. Liu, Label-free electrochemical aptasensor based on magnetic α-Fe2O3/Fe3O4 heterogeneous hollow nanorods for the detection of cancer antigen 125, Bioelectrochemistry 148 (2022), 108255.
[197] D. Hu, H. Cui, X. Wang, F. Luo, B. Qiu, W. Cai, H. Huang, J. Wang, Z. Lin, Highly sensitive and selective photoelectrochemical aptasensors for cancer biomarkers based on MoS2/Au/GaN photoelectrodes, Anal. Chem. 93 (19) (2021) 7341–7347.
[198] F. Fazlali, P. Hashemi, S.M. Khoshfetrat, R. Halabian, B. Baradaran, M. Johari-Ahar, P. Karami, A. Hajian, H. Bagheri, Electrochemiluminescent biosensor for ultrasensitive detection of lymphoma at the early stage using CD20 markers as B cell-specific antigens, Bioelectrochemistry 138 (2021), 107730.
[199] C. Hu, G. Wei, F. Zhu, A. Wu, L. Luo, S. Shen, J. Zhang, Platinum-based nanocomposite Pt@BSA as an efficient electrochemical biosensing interface for rapid and ultrasensitive determination of folate receptor-positive tumor cells, ACS Appl. Bio Mater. 5 (6) (2022) 3038–3048.
[200] J. Liu, M. Wang, C. Zhang, G. Li, Q. Shen, L. Zou, An ingenious electrochemical aptasensor for detection of CYFRA 21–1 based on dual-output toehold mediated strand displacement reaction, Bioelectrochemistry 147 (2022), 108203.
[201] Q. Wu, W. Zheng, A highly sensitive electrochemiluminescence sensor based on antimony tin oxide/TiO2 for detection of gastrin-releasing peptide (ProGRP), Int. J. Electrochem. Sci. 17 (221188) (2022) 2.
[202] C.P. Kurup, N.F. Mohd-Naim, N.A. Keasberry, S.N.A. Zakaria, V. Bansal, M. U. Ahmed, Label-free electrochemiluminescence nano-aptasensor for the ultrasensitive detection of ApoA1 in human serum, ACS Omega 7 (43) (2022) 38709–38716.
[203] Y. Zhang, N. Li, Y. Xu, X. Liu, Y. Ma, Z. Huang, H. Luo, C. Hou, D. Huo, A novel electrochemical biosensor based on AMNFs@ZIF-67 nano composite material for ultrasensitive detection of HER2, Bioelectrochemistry 150 (2023), 108362.
[204] Y. Zhao, Q. Liu, Y. Qin, Y. Cao, J. Zhao, K. Zhang, Y. Cao, Ordered labeling-facilitated electrochemical assay of alpha-fetoprotein-L3 ratio for diagnosing hepatocellular carcinoma, ACS Appl. Mater. Interfaces 15 (5) (2023) 6411–6419.
[205] Y. Zhang, Y. Xu, N. Li, N. Qi, L. Peng, M. Yang, C. Hou, D. Huo, An ultrasensitive dual-signal ratio electrochemical aptamer biosensor for the detection of HER2, Colloids Surf. B Biointerfaces 222 (2023), 113118.
[206] Y. Zhang, N. Li, Y. Xu, M. Yang, X. Luo, C. Hou, D. Huo, An ultra-sensitive electrochemical aptasensor based on Co-MOF/ZIF-8 nano-thin-film by the in-situ electrochemical synthesis for simultaneous detection of multiple biomarkers of breast cancer, Microchem. J. 187 (2023), 108316.
[207] Y. Liu, S. Huang, J. Li, M. Wang, C. Wang, B. Hu, N. Zhou, Z. Zhang, 0D/2D heteronanostructure–integrated bimetallic CoCu-ZIF nanosheets and MXene-derived carbon dots for impedimetric cytosensing of melanoma B16-F10 cells, Microchim. Acta 188 (3) (2021) 69.
[208] S. Lee, S. Hayati, S. Kim, H.J. Lee, Determination of protein tyrosine kinase-7 concentration using electrocatalytic reaction and an aptamer-antibody sandwich assay platform, Catal. Today 359 (2021) 76–82.